*Zoological Studies* **62**:21 (2023)
doi:10.6620/ZS.2023.62-21

Zoological Studies

Open Access

# Molecular and Morphological Characterizations of the Fish Parasitic Isopod *Mothocya parvostis* (Crustacea: Cymothoidae) Parasitizing Optional Intermediate Hosts: Juveniles of the Cobaltcap Silverside *Hypoatherina tsurugae* and Yellowfin Seabream *Acanthopagrus latus*

**Hiroki Fujita[1,*], Kentaro Kawai[1], Diego Deville[1], and Tetsuya Umino[1]**

[1]*Graduate School of Integrated Sciences for Life, Hiroshima University, 1-4-4 Kagamiyama, Higashi-Hiroshima, Hiroshima 739-8528, Japan.*
**Correspondence: E-mail: hirokifujita1231@gmail.com (Fujita).*
*E-mail: kawai-ken@hiroshima-u.ac.jp (Kawai); diegodeville1608@gmail.com (Deville); umino@hiroshima-u.ac.jp (Umino)*

Received 16 June 2022 / Accepted 10 February 2023 / Published 22 May 2023
Communicated by Benny K.K. Chan

*Mothocya parvostis* (Isopoda: Cymothoidae) is a parasitic crustacean that infests the opercular cavities of fishes. Its main final host is the Japanese halfbeak, *Hyporhamphus sajori*. However, *M. parvostis* also infests the black sea bream, *Acanthopagrus schelgelii*, as an optional intermediate host. Understanding the use of optional intermediate hosts is important for understanding the life history of Cymothoidae, and further information should be obtained. In this study, we aim to investigate the life cycle of *M. parvostis*. We collected and examined 20 mancae and 144 juveniles of *M. parvostis* from 129 cobaltcap silversides, *Hypoatherina tsurugae*, and 494 yellowfin seabreams, *Acanthopagrus latus*. Molecular analysis of the cytochrome *c* oxidase subunit I gene and 16S rRNA genes revealed that cymothoid mancae and juveniles from the two fish species were identified to be *M. parvostis*. All *M. parvostis* on *H. tsurugae* and *A. latus* might be mancae or juveniles, with no adult parasites; thus, *H. tsurugae* and *A. latus* juveniles were optional intermediate hosts of *M. parvostis*. In the results of morphological description, *M. parvostis* juveniles infesting the final host *H. sajori* lacked swimming setae, while juveniles parasitizing the two optional intermediate hosts had them. *Mothocya parvostis* mancae infested juveniles of both species just after metamorphosis, grew with the host. As the fish grows further, the parasite detached from the fish. The parasitic status of *M. parvostis* in the three optional intermediate hosts indicated that *M. parvostis* likely reproduced from June to December, and different optional intermediate hosts were used depending on the time of year in Hiroshima Bay. Therefore, a parasitic strategy involving optional intermediate hosts might increase the infestation success of *M. parvostis* to *H. sajori*.

**Key words:** Life cycle, Manca, New host record, Parasitic cymothoid, Prevalence.

## BACKGROUND

Cymothoidae Leach, 1818 includes 363 species under 42 genera of cosmopolitan isopod parasites (Boyko et al. 2008 onwards). Their hosts include diverse taxa of fish inhabiting marine, brackish, and freshwater

Citation: Fujita H, Kawai K, Deville D, Umino T. 2023. Molecular and morphological characterizations of the fish parasitic isopod *Mothocya parvostis* (Crustacea: Cymothoidae) parasitizing optional intermediate hosts: juveniles of the cobaltcap silverside *Hypoatherina tsurugae* and yellowfin seabream *Acanthopagrus latus*. Zool Stud **62**:21. doi:10.6620/ZS.2023.62-21.

environments (Yamauchi 2016). These parasites attach to their hosts at four sites: the opercular cavity, buccal cavity, abdominal cavity, and body surface (Smit et al. 2014; Aneesh et al. 2021). Cymothoids have six life stages (Brusca 1978a b 1981; Smit et al. 2014; Aneesh et al. 2015 2016 2018; Aneesh and Kappalli 2020), but are mainly identified on the basis of the morphological characteristics of adult females; thus, morphology-based species identification is difficult, and molecular analysis is the only way to identify non-female specimens (Fujita et al. 2021).

Free-swimming mancae (larvae) grow into juveniles and adult males on the hosts, and then adult cymothoids change sex from male to female (Brusca 1978a b 1981; Smit et al. 2014; Aneesh et al. 2015 2016 2018; Aneesh and Kappalli 2020). Mancae of cymothoids search for hosts in a free-swimming stage. Once a host is found, they develop into juveniles. However, free-swimming juveniles of *Mothocya*, *Nerocila*, and *Anilocra* have been collected (Saito et al. 2014).

Mancae and juveniles of some cymothoid species, such as *Anilocra clupei* Williams & Bunkley-Williams, 1986, *A. pomacentri* Bruce, 1987, *Mothocya parvostis* Bruce, 1986, *Nerocila acuminata* Schioedte and Meinert, 1881, *Olencira praegustator* (Latrobe, 1802), and *Telotha henselii* (Martens, 1869), temporarily infest fishes other than their final hosts (Adlard and Lester 1995; Lindsay and Moran 1976; Segal 1987; Taberner et al. 2003; Fogelman and Grutter 2008; Fujita et al. 2020; Fujita 2022); these hosts are called "optional intermediate hosts." These intermediate hosts are

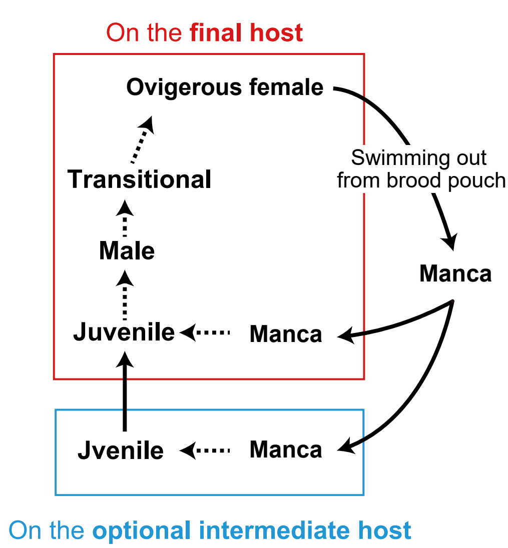


**Fig. 1.** Diagram of cymothoid life cycles including optional intermediate and final hosts. Solid lines indicate migration by free-swimming and broken lines indicate development of cymothoids.

"optional" because they are not necessary in a parasite's normal life cycle (Fig. 1). Also, free-swimming juveniles were collected, presumably after leaving the optional intermediate hosts (Fujita et al. 2023). *Mothocya parvostis* is a common Cymothoidae in Japan which infests the Japanese halfbeak *Hyporhamphus sajori* (Temminck and Schlegel, 1846), large-scale blackfish *Girella punctata* Gray, 1835, and Japanese amberjack *Seriola quinqueradiata* Temminck and Schlegel, 1845 as final hosts (Bruce 1986). A major final host is *H. sajori* (Nagasawa 2020), and it shows a high prevalence of approximately 50% (Kawanishi et al. 2016; Fujita et al. 2020). In Hiroshima Bay, *M. parvostis* infests juveniles of the black sea bream *Acanthopagrus schlegelii* (Bleeker, 1854), as an optional intermediate host (Fujita et al. 2020). The presence of optional intermediate hosts has not been examined in species other than *A. schlegelii*.

The reproduction cycles of Cymothoidae organisms vary. *Anilocra pomacentri* has no fixed reproduction season and reproduces throughout the year (Adlard and Lester 1995), and *Mothocya epimerica* Costa, 1851 has four reproduction seasons per year (Bello et al. 1997). The reproduction cycles of *M. parvostis* are unknown. So, there is a possibility that juvenile fishes that appear in other seasons may be used as optional intermediate hosts. Thus, we focused on juveniles of the yellowfin seabream *Acanthopagrus latus* (Houttuyn, 1782), a related species of *A. schlegelii* that appears in Hiroshima Bay in different seasons than *A. schelgelii*. *Acanthopagrus latus* is as recreationally and commercially important in the Indo-West Pacific region as *A. schlegelii* (Iwatsuki 2013). One of the most significant ecological differences between *A. latus* and *A. schlegelii* is their spawning season. In particular, *A. latus* spawns in autumn (Abol-Munafi and Umeda 1994; Nishida 2022), whereas *A. schlegelii* spawns in spring (Kawai et al. 2017 2020 2021). We also focused on the juveniles of cobaltcap silverside *Hypoatherina tsurugae* (Jordan and Starks, 1901), which grow in the period between the growth seasons of *A. schlegelii* and *A. latus*. *Hypoatherina tsurugae* serves as a food source for various carnivorous fishes (Mori et al. 1988) and is used for recreational fishing. Its spawning season in coastal Japan is from May to July, and the juveniles are collected from June to October (Mori et al. 1988).

In this study, we performed DNA analysis to identify the cymothoids infesting juveniles of *H. tsurugae* and *A. latus* as *M. parvostis*. In addition, we morphologically describe *M. parvostis* mancae and juveniles infesting *H. tsurugae* and *A. latus* to compare them with those infesting *H. sajori*. *Mothocya parvostis* infested these two species in different seasons from its infestation in *A. schlegelii*; thus, we updated our knowledge about the optional intermediate hosts and parasitic strategies of *M. parvostis*.

## MATERIALS AND METHODS

### Sample Collection

A total of 129 *H. tsurugae* and 494 *A. latus* juveniles were collected between 6 July 2021 and 14 October 2021, and between 27 October 2021 and 8 January 2022. Sampling was performed using hand, surf, and casting nets on the coast of Nomijima Island, Hiroshima Bay, Seto Inland Sea, Japan. In the case of *H. tsurugae*, individuals smaller than 75 mm, which corresponds to zero age (Mori et al. 1988), were considered juveniles. In the case of *A. latus*, individuals smaller than 160 mm were considered juveniles because they were qualified as immature (Hesp et al. 2004). Parasites infesting *H. sajori* were collected for morphological comparison between 26 November 2020 and 29 March 2021 in Hiroshima. Mancae swimming out from a blood pouch of ovigerous female infesting *H. sajori* were collected on 29 October 2020 in Hiroshima. The collected samples were preserved in 99.5% ethanol.

The standard length (SL) of the fish and total length (TL) of the cymothoids were measured. The prevalence of *M. parvostis* to *H. tsurugae* and *A. latus* was calculated by dividing the number of the infested fishes by the total number of collected fishes. The "manca-prevalence" and "juvenile-prevalence" was calculated by dividing the number of fishes infested at each respective cymothoid stage by the total number of the collected fishes of *H. tsurugae* and *A. latus*. If a single fish was infested by mancae and juveniles, it was included in the estimation of both manca- and juvenile-prevalence.

### Molecular identification

A total of 20 cymothoids from *H. tsurugae* juveniles and 19 cymothoids from *A. latus* juveniles were randomly selected for molecular analyses. Total DNA was isolated from pereopods via an alkaline lysis method (Toyobo 2012). Eighteen microliters of NaOH (50 mM) was added to the pereopod and incubated at 95°C for 10 min. Next, 2 μL Tris-HCl (1 M, pH 8.0) was added, and the tube was vortexed thoroughly and centrifuged at 12,000 rpm for 5 min. The supernatant was removed and stored at -30°C until use in PCR.

Analyses and species identification were performed following Fujita et al. (2020). Partial cytochrome *c* oxidase subunit I gene (*COI*) sequences were amplified using the primers LCO1490 (5'-GGTCAACAAATCATAAAGATATTGG-3') and HCO2198 (5'-TAAACTTCAGGGTGACCAAAAAATCA-3') (Folmer et al. 1994), and partial 16S rRNA sequences were amplified using the primers 16Sar (5'-CGCCTGTTTAACAAAAACAT-3') and 16Sbr (5'-CCGGTCTGAACTCAGATCATGT-3') (Simon et al. 1994). The total volume for each PCR was 8.1 μL, which was composed of 1 μL of DNA, 0.78 μL of ultrapure water, 4.06 μL of 2× PCR buffer, 1.62 μL of dNTP mix, 0.24 μL of each primer (10 μM solutions), and 0.16 μL of KOD FX Neo DNA polymerase (Toyobo, Osaka, Japan). The thermocycler profile of *COI* involved an initial denaturation at 94°C for 2 min; 30 cycles of denaturation at 98°C for 10 s, annealing at 50°C for 45 s, and extension at 68°C for 30 s; and a final extension at 68°C for 7 min. The thermocycler profile of 16S rRNA consisted of an initial denaturation at 94°C for 2 min; 30 cycles of denaturation at 98°C for 10 s, annealing at 50.5°C for 30 s, and extension at 68°C; and a final extension at 68°C for 7 min. The PCR products were sequenced via the dye terminator method using an ABI 3130xl genetic analyzer (Applied Biosystems, CA, USA).

The sequences were aligned using MUSCLE (Edgar et al. 2004), implemented in MEGA 10 (Kumar et al. 2018), trimmed, and collapsed into haplotypes. All sequences were deposited into GenBank (accession numbers: LC757644–LC757691). Additional sequences belonging to *Mothocya*, which is distributed in Japan, were downloaded from GenBank (Table S1). The sequences of *Anilocra* Leach, 1818, *Ceratothoa* Dana, 1852, and *Nerocila* Leach, 1818, which are relative genera of *Mothocya* within Cymothoidae (Hata et al. 2017) that inhabit the waters of Japan (Table S1), were included to compare genetic distances within and between species. Pairwise intra- and interspecific genetic distances with the Kimura two-parameter (K2P) model (Kimura 1980) were calculated using MEGA10, and a neighbor-joining tree (Saitou and Nei 1987) was generated using *COI* and 16S rRNA sequences. *Ichthyoxenos japonensis* Richardson, 1913 (NC 039713 and MF419233) were also included as outgroups.

### Morphological description

Morphological descriptions were made with the aid of an SZX7 and BX50 (Olympus, Tokyo, Japan). Drawings were digitally inked using Illustrator (version 26.5) (Adobe, CA, USA) and DTC133 pen display (Wacom, Saitama, Japan). Measurements and terminologies essentially follow Aneesh et al. (2019a b 2020). The life stages of the cymothoids were divided into mancae, juveniles, and adults, following Aneesh et al. (2016) and Fujita (2022).

## RESULTS

### Cymothoids infesting *H. tsurugae*

In this study, six mancae and 14 juveniles of Cymothoidae were collected from the opercular cavities of 129 *H. tsurugae* juveniles (Figs. 2 and 3). Of the 16 infested fishes, only three were simultaneously infested by more than two cymothoid individuals. The SL of *H. tsurugae* juveniles increased with each sampling day (Fig. 4); however, the TL of cymothoids did not significantly correlate with the SL of *H. tsurugae* juveniles (Fig. 5). The prevalence of cymothoids in *H. tsurugae* increased with each sampling day and reached a maximum of 20.8% (Fig. 6). The manca-prevalence did not change significantly during the sampling season, but the juvenile-prevalence increased (Fig. 6). The manca-prevalence in small fish (< 20 mm) was 50%, and decreased in larger fish. The juvenile-prevalence increased with larger fish (Fig. 7).

### Cymothoids infesting *A. latus*

A total of 80 mancae and 64 juveniles of Cymothoidae were collected from the opercular cavity of 494 *A. latus* juveniles (Figs. 2 and 3). Of the 138 infested fishes, only seven were simultaneously infested by more than two cymothoid individuals. The SL of *A. latus* juveniles increased with each sampling day (Fig. 4). The TL of cymothoids was significantly correlated with the SL of *A. latus* juveniles (Fig. 5). The prevalence of cymothoids in *A. latus* did not significantly change during the sampling period (Fig. 6). However, after mid-December, the manca-prevalence decreased, whereas the juvenile-prevalence increased, and all cymothoids identified in early January were juveniles (Fig. 6). The manca-prevalence in small fish (< 10 mm) was 33.3%, and decreased in larger fish. The juvenile-prevalence increased in larger fish. Almost all cymothoids infesting large *A. latus* juveniles (> 20 mm) were juveniles (Fig. 7).

### Molecular identification

Our alignment matrices of the *COI* and 16S rRNA genes consisted of 594 and 412 bp, representing seven and eight haplotypes, respectively. Our neighbor-joining tree with *COI* and 16S rRNA genes showed that

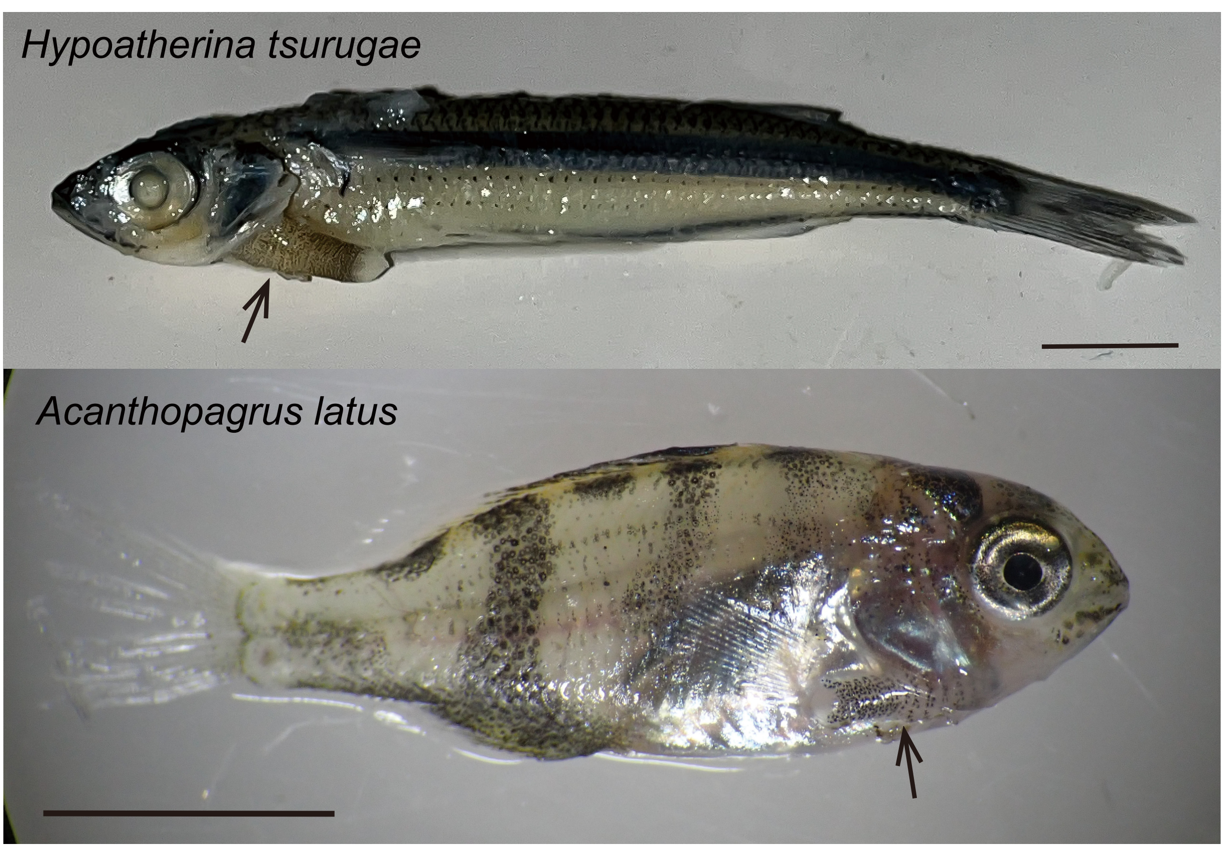


**Fig. 2.** Juveniles of cobaltcap silverside *Hypoatherina tsurugae* and yellowfin seabream *Acanthopagrus latus* infested with *Mothocya parvostis.* Arrows indicate *M. parvostis.* Scale bars = 5 mm.

all haplotypes detected from cymothoids infesting *H. tsurugae* and *A. latus* formed a well-supported clade, along with the sequence identified as *M. parvostis* by Hata et al. (2017) and Fujita et al. (2020) (Fig. 8). Pairwise intra- and interspecific genetic distances with the *COI* and 16S rRNA haplotypes revealed that the intraspecific distances were smaller than the interspecific distances (Tables 1 and 2), but they did not overlap. The minimum interspecific distances within *Mothocya* were 3.1% (*COI*) and 1.9% (16S rRNA) before and after the inclusion of haplotypes from this study. The maximum distances between our haplotypes were 1.0% (*COI*) and 0.8% (16S rRNA). These values were comparable with the intra- and interspecific distances of *Anilocra*, *Cerathothoa*, and *Nerocila* (Tables 1 and 2).

## Morphological description

**Family Cymothoidae Leach, 1818**
**Genus *Mothocya* Costa, 1851**
***Mothocya parvostis* Bruce, 1986**
(Figs. 2, 3, 9–16)

*Material examined*: Juvenile (TL 7.19 mm), from the coast of Nomijima Island, Hiroshima Bay, Seto Inland Sea, Japan, 34°13'49.6"N 132°23'18.4"E, in a opercular cavity of juvenile of *Hypoatherina tsurugae* (SL: 50.84 mm), 14 October 2021, coll. H. Fujita. Juvenile (TL 6.89 mm), from the coast of Nomijima Island, Hiroshima Bay, Seto Inland Sea, Japan, 34°11'43.3"N 132°26'33.4"E, collected in a opercular

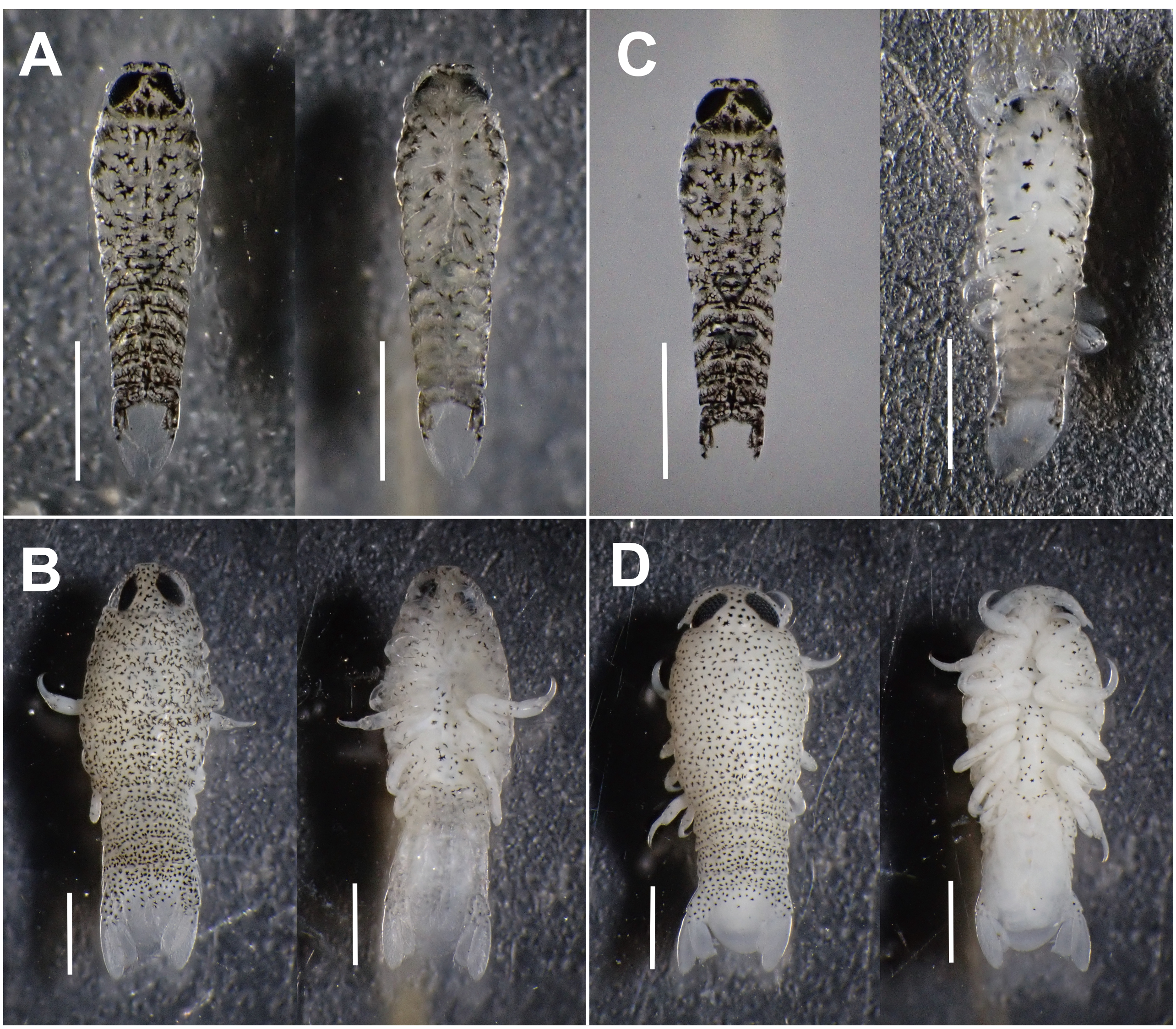


**Fig. 3.** Dorsal and ventral views of *Mothocya parvostis* infesting juveniles of cobaltcap silverside *Hypoatherina tsurugae* (A and B) and yellowfin seabream *Acanthopagrus latus* (C and D). A and C: mancae, B and D: *M. parvostis* juveniles. Scale bars = 1 mm.

cavity of juvenile of *Acanthopagrus schelgelii* (SL: 23.27 mm), 8 January 2022, coll. H. Fujita. Manca (TL 3.12 mm), from the coast of Nomijima Island, Hiroshima Bay, Seto Inland Sea, Japan, 34°13'49.6"N 132°23'18.4"E, collected in a opercular cavity of juvenile of *Hypoatherina tsurugae* (SL: 14.5 mm), 6 July 2021, coll. H. Fujita. Manca (TL 2.96 mm), from the coast of Nomijima Island, Hiroshima Bay, Seto Inland Sea, Japan, 34°11'43.3"N 132°26'33.4"E, collected in a opercular cavity of juvenile of *Acanthopagrus schelgelii* (SL: 12.22 mm), 27 October 2021, coll. H. Fujita.

Description of juvenile infesting *H. tsurugae* (Figs. 9, 10): Body elliptical, 2.9–3.0 times as long as greatest width, dorsal surfaces convex, widest at pereonite 5, most narrow at pleonite 1. Cephalon 1.4 times wider than long, semi triangle, slightly immersed in pereonite 1. Anterior margin produced moderately rostrum. Eyes oval with distinct margins, one eye 0.3–0.4 times width of cephalon; 0.3–0.8 times length of cephalon.

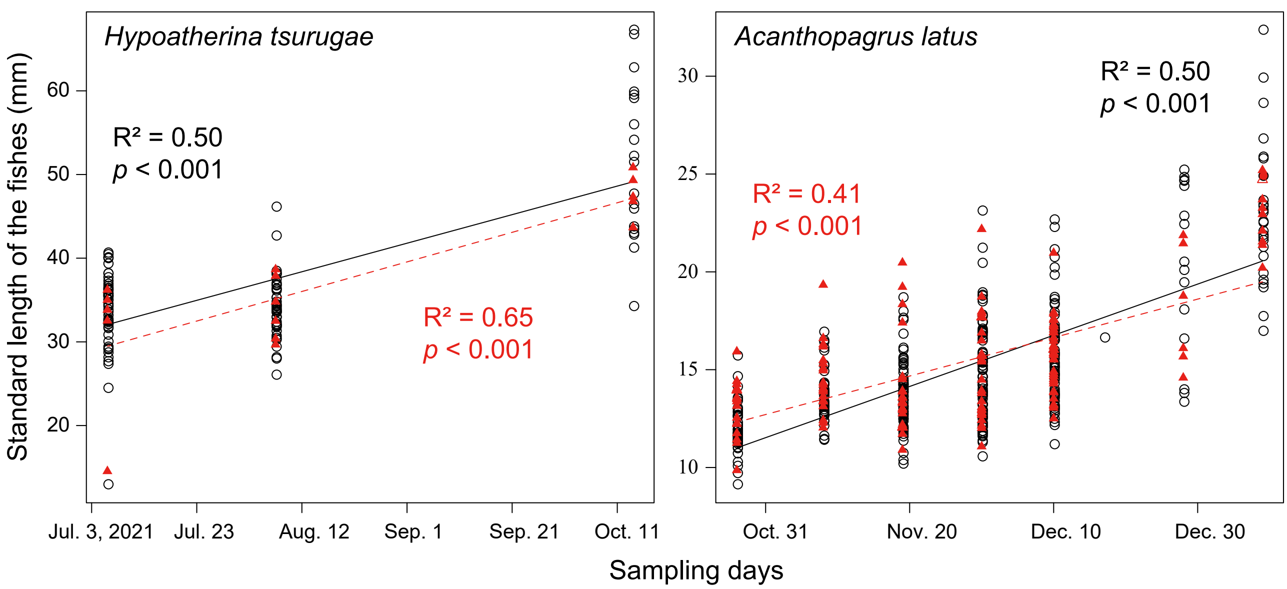


**Fig. 4.** Scatter plots of the standard length of non-infested and infested fish for each sampling date in juveniles of cobaltcap silverside *Hypoatherina tsurugae* and yellowfin seabream *Acanthopagrus latus*. The open circles (black) indicate non-infested fish, and the closed triangles (red) indicate infested fish. The solid lines (black) for non-infested fishes and the broken lines (red) for infested fishes are regression lines.

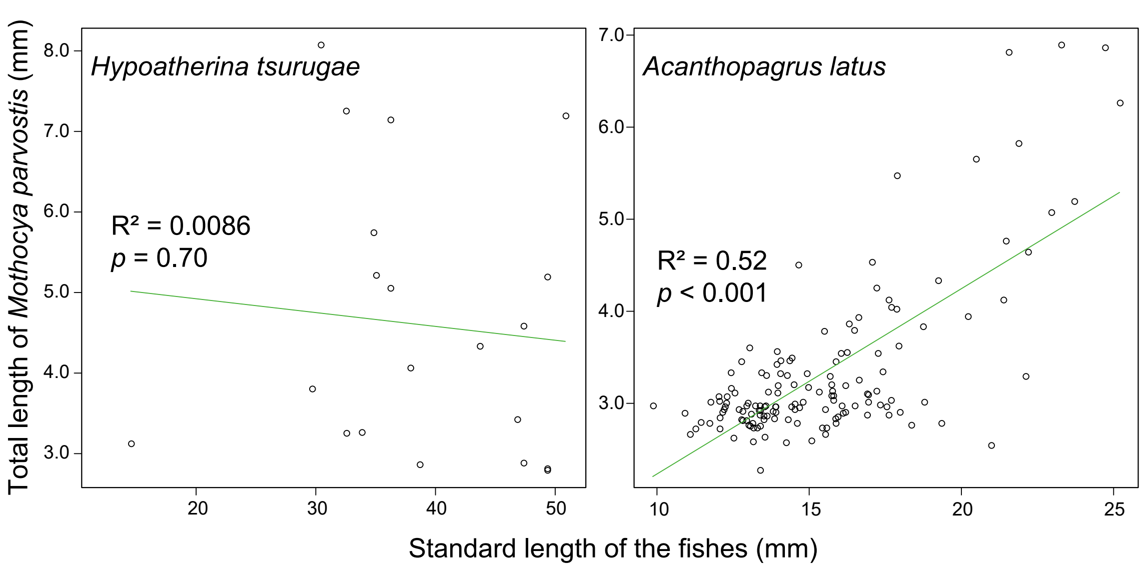


**Fig. 5.** Scatter plots of the standard length of fishes and the total length of *M. parvostis* in juveniles of cobaltcap silverside *Hypoatherina tsurugae* and yellowfin seabream *Acanthopagrus latus*. The solid lines are regression lines.

Pereonite 1 anterior border medially straight, slightly curved laterally. Coxae 2–7 slightly visible or invisible in dorsal view; coxae strongly narrow. Pereonites 5 longest, pereonite 7 shortest; posterior margins smooth, slightly curved laterally; pereonites 7 with slightly recessed posterior margin. Pleon 0.2 times as total length, pleonites all visible in dorsal view, pleon 0.7–0.8 times as wide as greatest body width. Pleotelson 0.8–0.9 times length as wide, 1.6–1.7 times as long as pleon, posterior margin with short marginal setae.

Antennula with 8 articles, reaching posterior margin of cephalon.

Antenna with 8 articles, beyond anterior margin of pereonite 1.

Pereopod 1, basis 1.5 times as long as greatest width; ischium 0.6 times as long as basis; merus 0.6

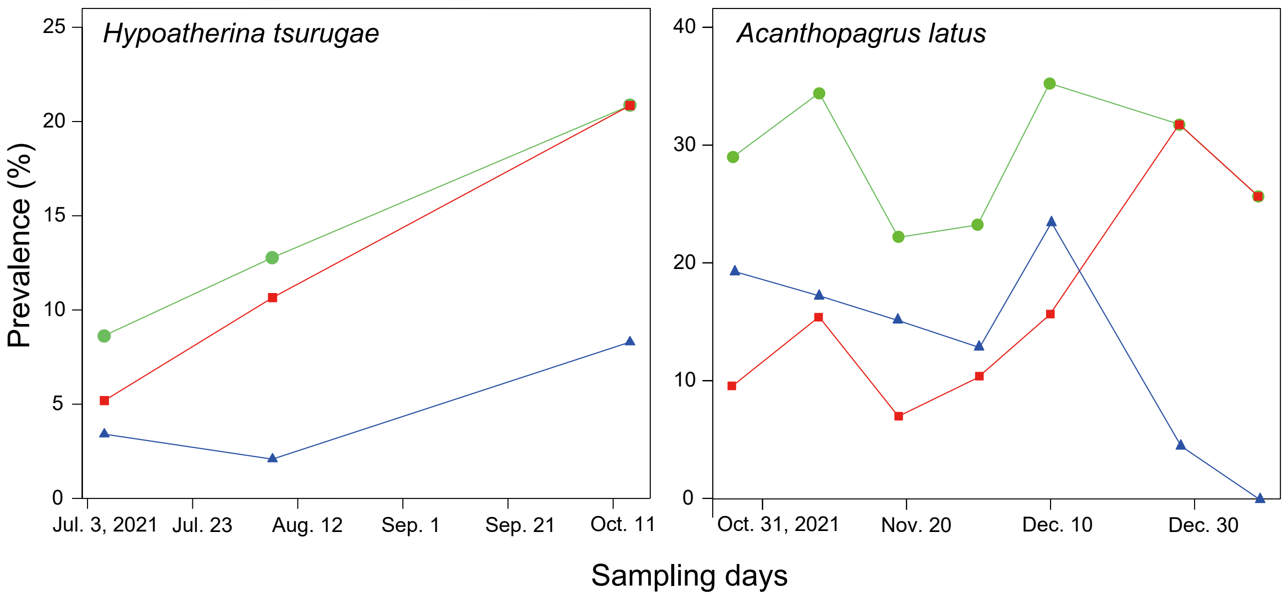


**Fig. 6.** Prevalence, manca-prevalence, and juvenile-prevalence for each sampling day in juveniles of cobaltcap silverside *Hypoatherina tsurugae* and yellowfin seabream *Acanthopagrus latus*. Closed circles (green), closed triangles (blue), and closed squares (red) indicate the prevalence, the manca-prevalence, and the juvenile-prevalence, respectively.

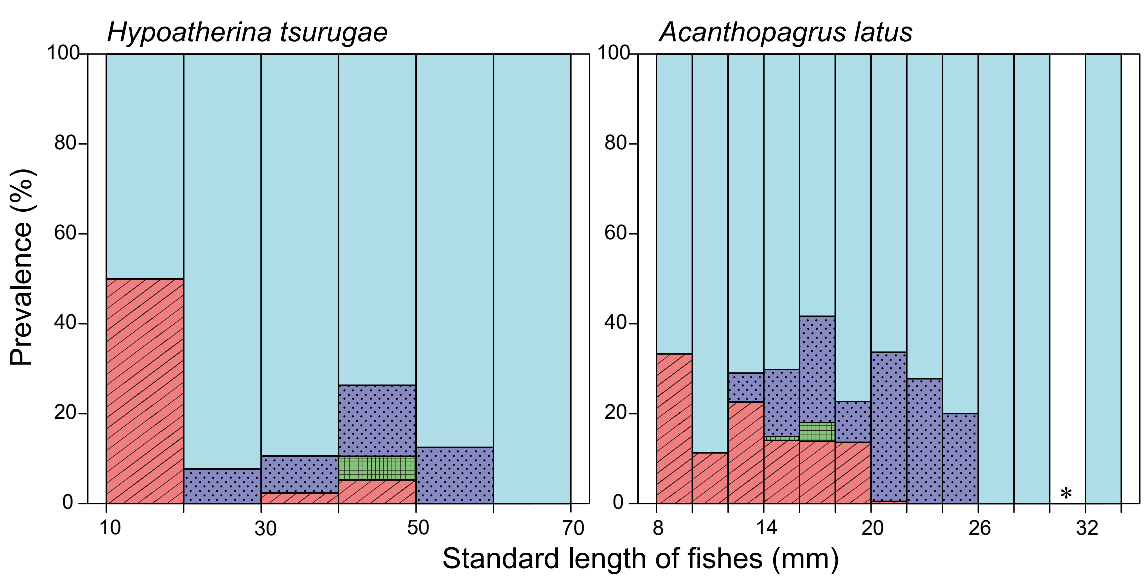


**Fig. 7.** Prevalence of the standard-length range of juveniles of cobaltcap silverside *Hypoatherina tsurugae* and yellowfin seabream *Acanthopagrus latus*. Diagonal shading bars (red), dot bars (blue), grid bars (green), and plain bars (light blue) indicate the manca-prevalence, juvenile-prevalence, the percentage of fish parasitised by both mancae and juveniles, and non-infested fishes, respectively. The asterisk indicates no data.

times as long as ischium; carpus 0.4 times as long as merus; propodus 5 times as long as carpus; dactylus 1.1 times as long as propodus. Pereopod 2 similar to pereopod 1. Pereopod 3, basis 1.7 times as long as greatest width; ischium 0.5 times as long as basis; merus 0.6 times as long as ischium; carpus 0.6 times as long as merus; propodus 3.3 times as long as carpus; dactylus 1.25 times as long as propodus. Pereopod 4, basis 1.8 times as long as greatest width; ischium 0.8 times as long as basis; merus 0.4 times as long as

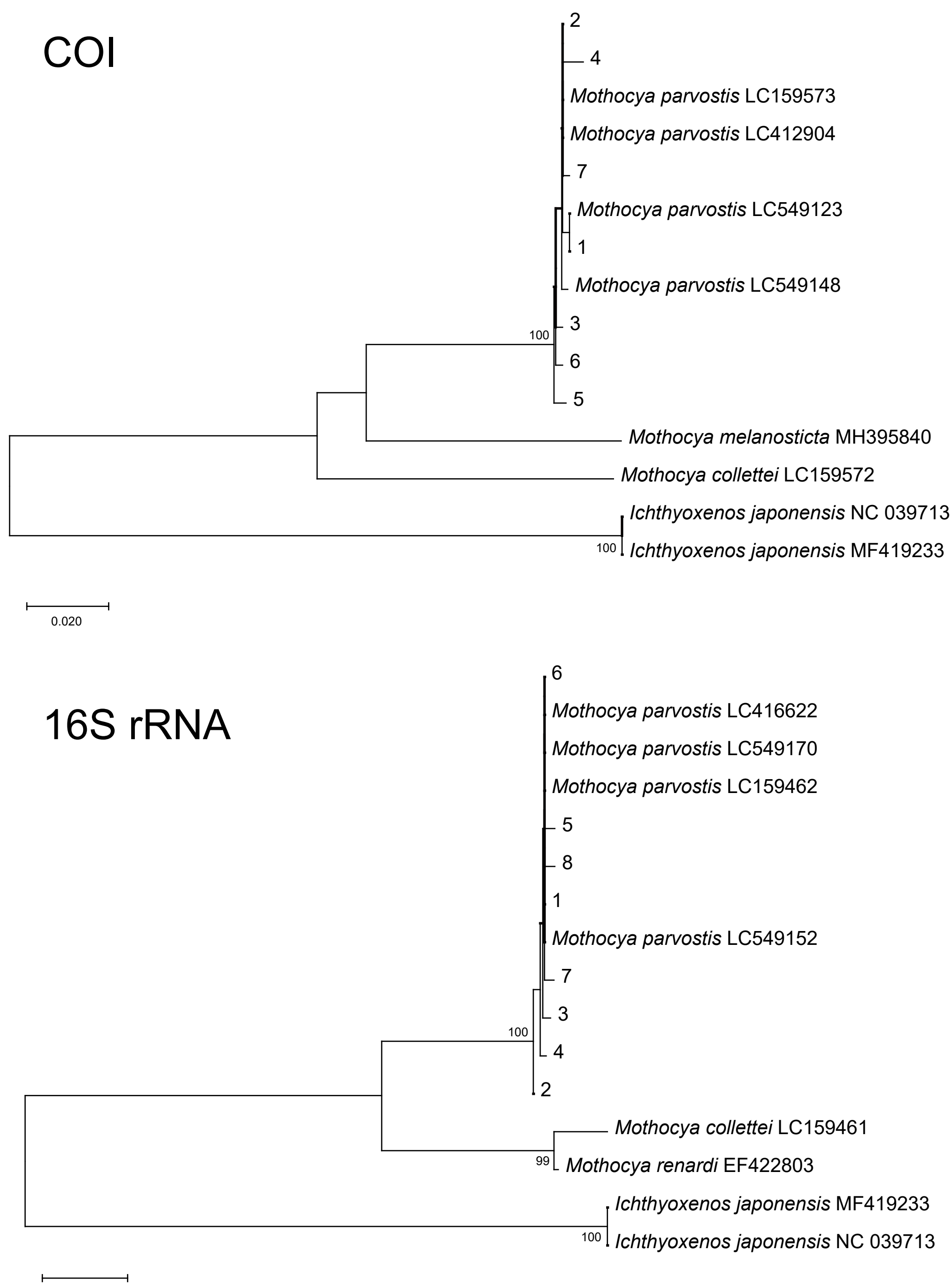


**Fig. 8.** Neighbor-joining trees showing seven and eight haplotypes of the cytochrome *c* oxidase subunit I (*COI*) and 16S rRNA gene infesting juveniles of cobaltcap silverside *Hypoatherina tsurugae* and yellowfin seabream *Acanthopagrus latus* along with selected sequences of other cymothoids downloaded from GenBank. Bootstrap values less than 98% are not shown. The accession numbers were deposited in GenBank (under registration).

ischium; carpus 1.0 times as long as merus; propodus 2.5 times as long as carpus; dactylus 1.1 times as long as propodus. Pereopods 5 and 6 similar to pereopod 4. No robust setae on pereopods 1–6. Pereopod 7, basis 2.3 times as long as greatest width; ischium 0.7 times as long as basis, 1 robust seta on inferior margin; merus 0.6 times as long as ischium; carpus 1.0 times as long as merus, 2 robust setae on inferior margin; propodus 1.7 times as long as carpus, 4 robust setae on inferior margin; dactylus 1.0 times as long as propodus.

Pleopods all lamellar, surface smooth. Pleopod 1 peduncle 1.7 times as wide as length, medial margin with 4 coupling hooks; endopod rectangular, 1.9 times as long as width; exopod trapezoidal, lateral margin almost straight, 1.9 times as long as width, 1.1 times as long as endopod, medial margin with short marginal setae. Pleopod 2 similar to pleopod 1; peduncle medial margin with 4 plumose setae; endopod with appendix masculina, slightly shorter than endopod.

Uropod rami beyond posterior margin of pleotelson; uropod, peduncle triangular, 0.7 times as long as exopod, 1.7 times as long as wide. Endopod oval, 2.3 times as long as greatest width, 0.8 times as long as exopod, lateral and medial margins with short marginal setae. Exopod semitriangular, 3.2 times as long as greatest width, medial margin with short marginal setae.

Description of juvenile infesting *A. latus* (Figs. 11, 12): Similar to juvenile infesting *H. tsurugae*. Body widest at pereonite 1–3, most narrow at pereonite 7. Pereonites 3 longest, pereonite 7 shortest. Each of pereopod 2 and 3 merus superior distal angle with 1 robust seta. Pereopod 6 propodus inferior margin with 1 robust seta. Pereopod 7 carpus and propodus with no robust seta. Pleopod 1 peduncle medial margin with 3 plumose setae.

Description of juvenile infesting *H. sajori*: Similar to juvenile infesting *H. tsurugae* and *A. latus*. Absence of marginal setae of pleotelson, pleopods and uropods.

Description of manca infesting *H. tsurugae* (Figs. 13, 14): Body elliptical, 3.4–4.1 times as long as greatest width, widest at pereonite 3, most narrow at pleonite 1. Pereonites 1 longest, pereonite 7 shortest; posterior margins straight. Pleon 0.3 times as total length, pleonites all visible in dorsal view, pleon 0.7–0.8 times as wide as greatest body width. Pleotelson 0.9–1.0 times as wide as length 0.7 times as long as pleon, posterior margin with marginal setae.

**Table 1.** Genetic distances determined using the Kimura two-parameter model for the cytochrome *c* oxidase subunit I gene (*COI*) sequences of Cymothoidae

| Comparison level | No. species | Intraspecific | | | Interspecific | | |
|---|---|---|---|---|---|---|---|
| | | Min. (%) | Max. (%) | Mean (%) | Min. (%) | Max. (%) | Mean (%) |
| Genus | | | | | | | |
| *Anilocra* | 2 | 0.000 | 0.349 | 0.202 | 10.959 | 11.187 | 11.028 |
| *Ceratothoa* | 4 | 0.169 | 2.593 | 1.221 | 18.398 | 31.589 | 29.224 |
| *Nerocila* | 2 | 0.000 | 1.280 | 0.444 | 27.307 | 28.836 | 27.721 |
| *Mothocya* | 4 | 0.000 | 1.020 | 0.261 | 3.126 | 13.902 | 11.752 |
| *Mothocya*[#] | 4 | 0.000 | 1.020 | 0.310 | 3.126 | 14.122 | 11.781 |

[#]Including haplotypes of *Mothocya parvostis* collected in the present study.

**Table 2.** Genetic distances obtained using the Kimura two-parameter model for the 16S rRNA gene sequences of Cymothoidae

| Comparison level | No. species | Intraspecific | | | Interspecific | | |
|---|---|---|---|---|---|---|---|
| | | Min. (%) | Max. (%) | Mean (%) | Min. (%) | Max. (%) | Mean (%) |
| Genus | | | | | | | |
| *Anilocra* | 2 | 1.328 | 1.875 | 1.622 | 18.940 | 19.715 | 19.327 |
| *Ceratothoa* | 3 | 0.000 | 1.229 | 0.643 | 14.043 | 24.881 | 22.661 |
| *Nerocila* | 2 | 0.000 | 1.050 | 0.638 | 20.564 | 20.564 | 20.564 |
| *Mothocya* | 3 | 0.000 | 0.836 | 0.219 | 1.003 | 9.994 | 9.356 |
| *Mothocya*[#] | 3 | 0.000 | 0.836 | 0.251 | 1.003 | 9.994 | 9.435 |

[#]Including haplotypes of *Mothocya parvostis* collected in the present study.

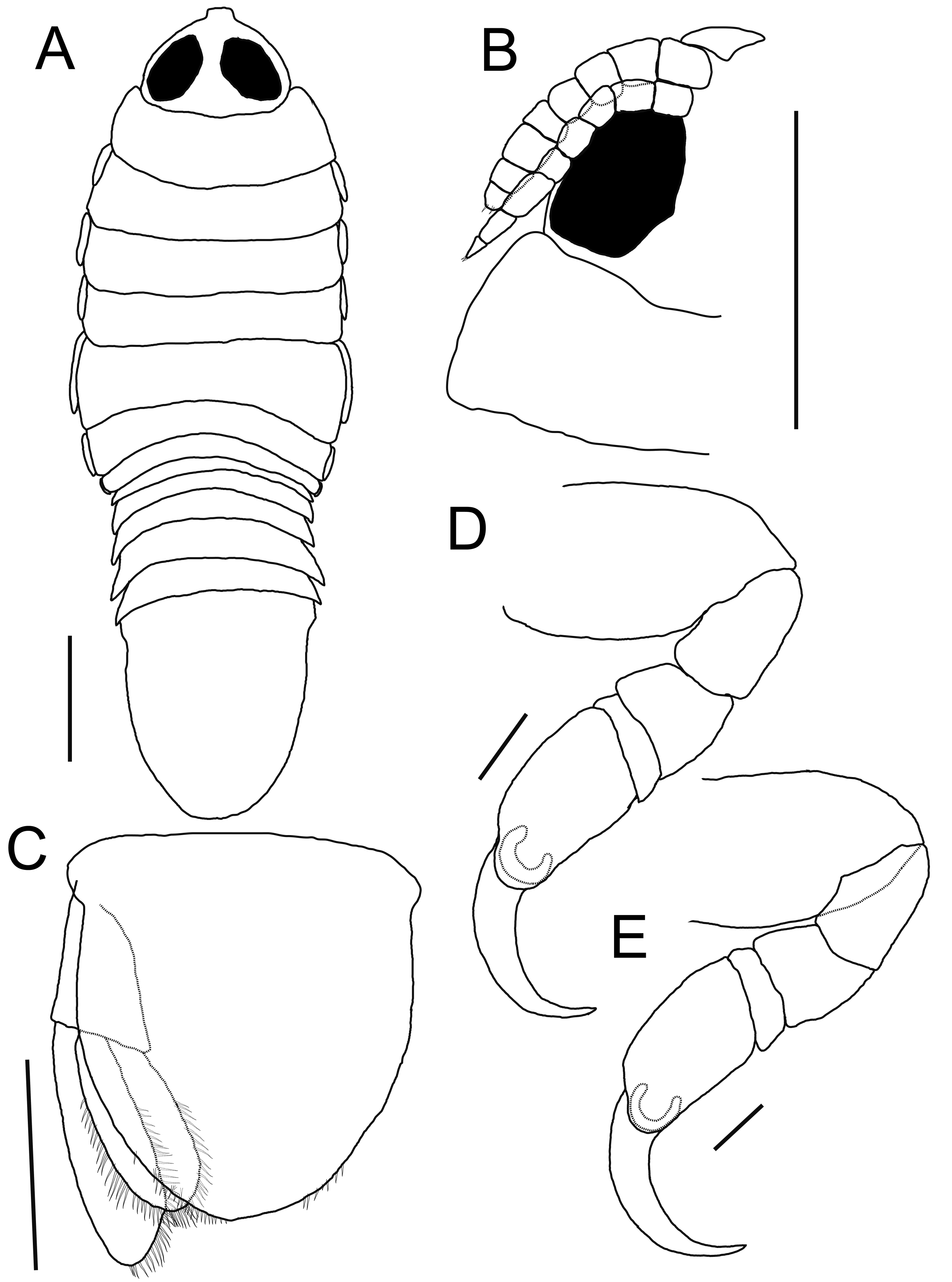


**Fig. 9.** *Mothocya parvostis* juvenile (7.19 mm) infesting a cobaltcap silverside *Hypoatherina tsurugae* juvenile (50.84 mm). (A) Body, dorsal view. (B) Cephalon, ventral view. (C) Pleotelson. (D, E) Pereopods 1, 2, respectively. Scale bars: A–C = 1 mm; D, E = 0.2 mm.

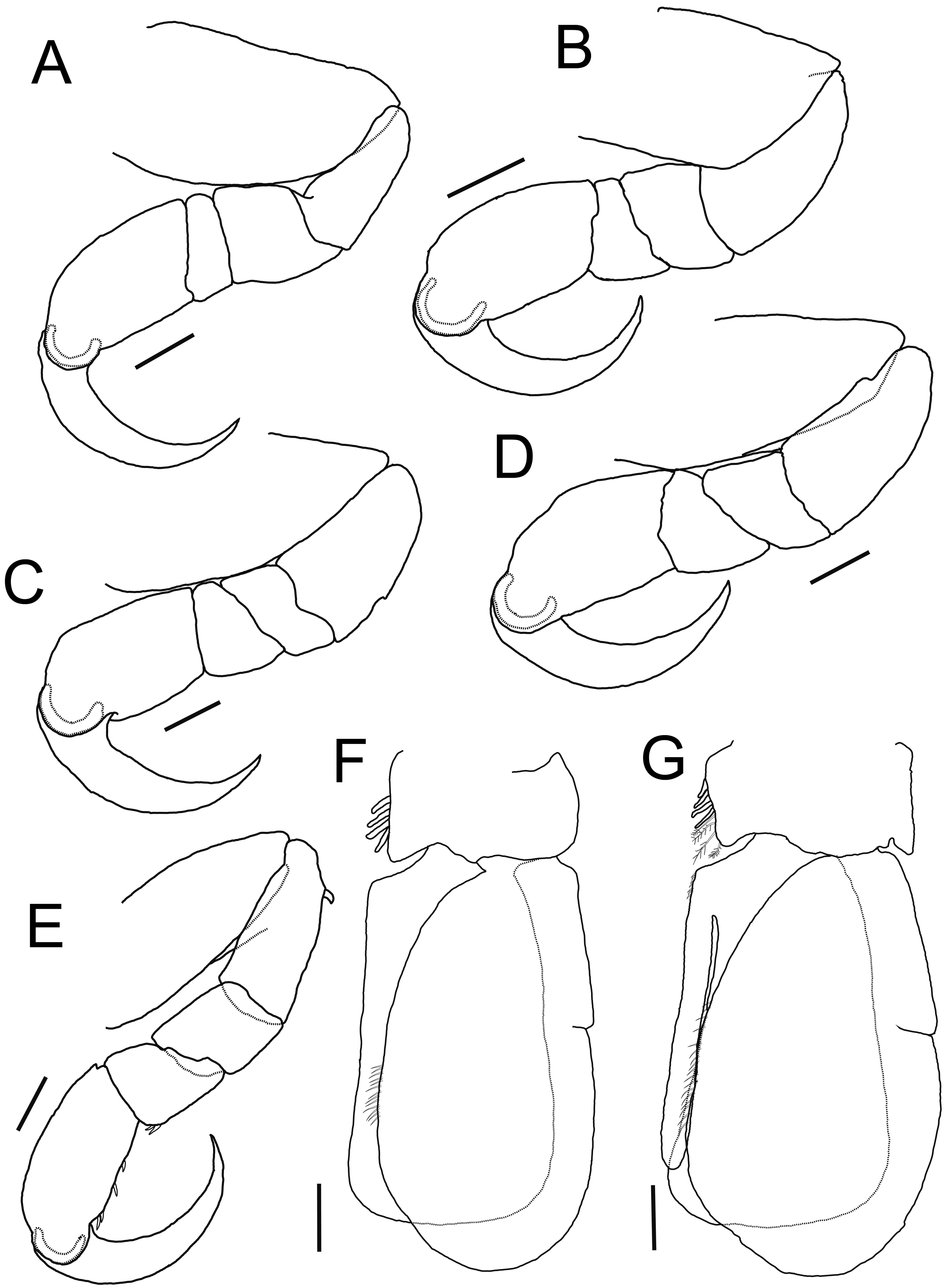


**Fig. 10.** *Mothocya parvostis* juvenile (7.19 mm) infesting a cobaltcap silverside *Hypoatherina tsurugae* juvenile (50.84 mm). (A–E) Pereopods 3–7, respectively. (F, G) Pleopods 1, 2, respectively. Scale bars = 0.2 mm.

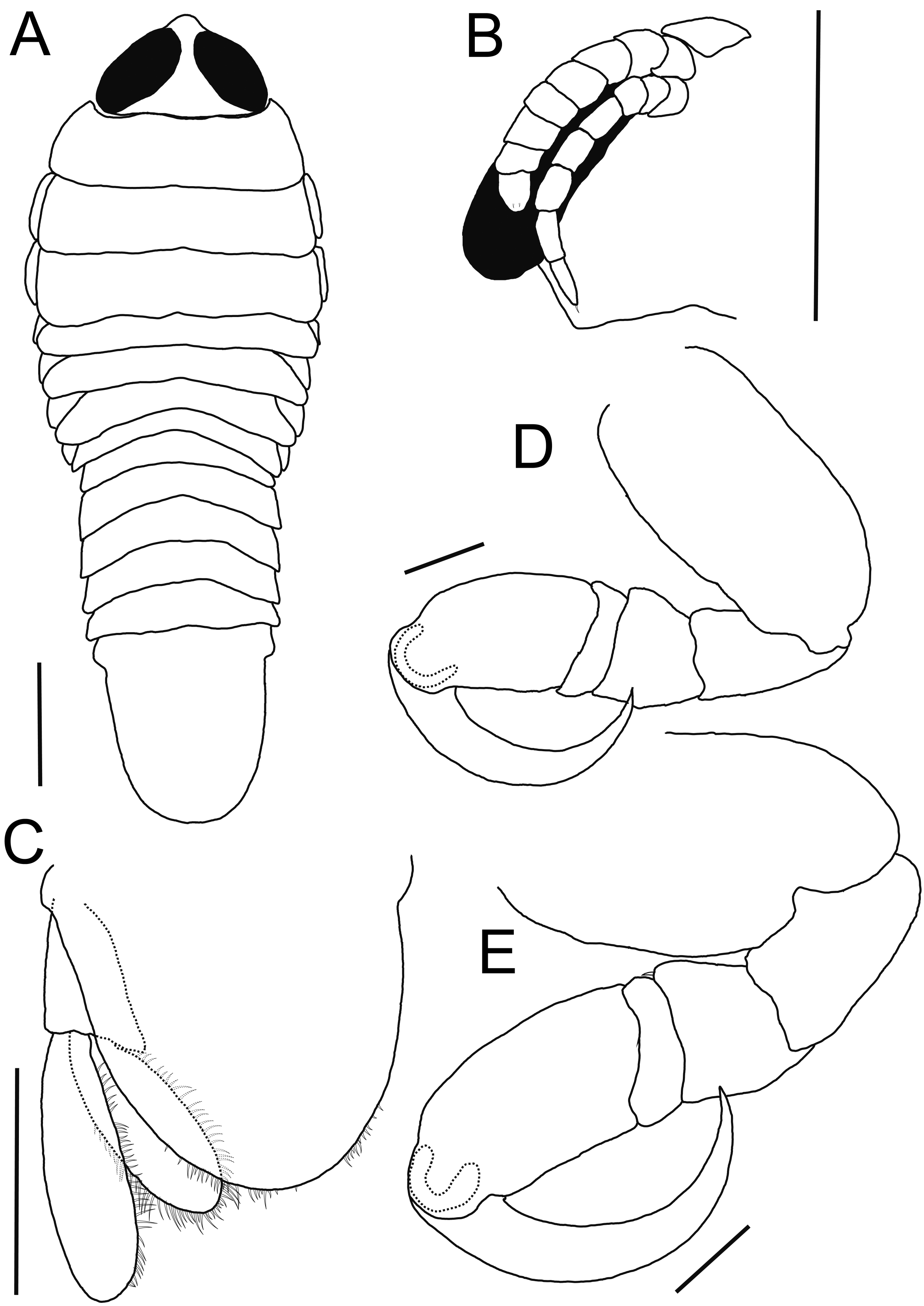


**Fig. 11.** *Mothocya parvostis* juvenile (6.89 mm) infesting a yellowfin seabream *Acanthopagrus latus* juvenile (23.27 mm). (A) Body, dorsal view. (B) Cephalon, ventral view. (C) Pleotelson. (D, E) Pereopods 1, 2, respectively. Scale bars: A–C = 1 mm; D, E = 0.2 mm.

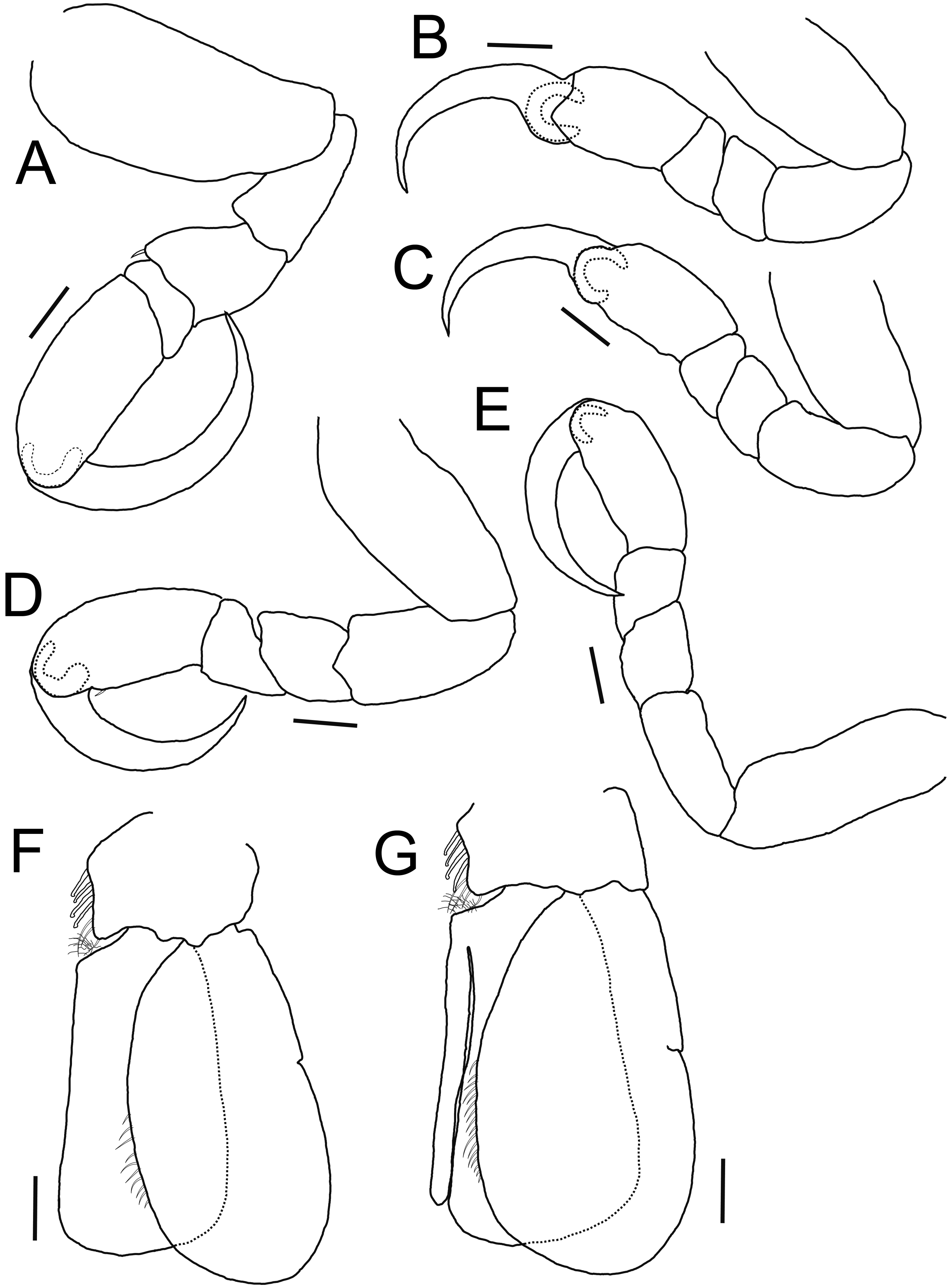


**Fig. 12.** *Mothocya parvostis* juvenile (6.89 mm) infesting a yellowfin seabream *Acanthopagrus latus* juvenile (23.27 mm). (A–E) Pereopods 3–7, respectively. (F, G) Pleopods 1, 2, respectively. Scale bars = 0.2 mm.

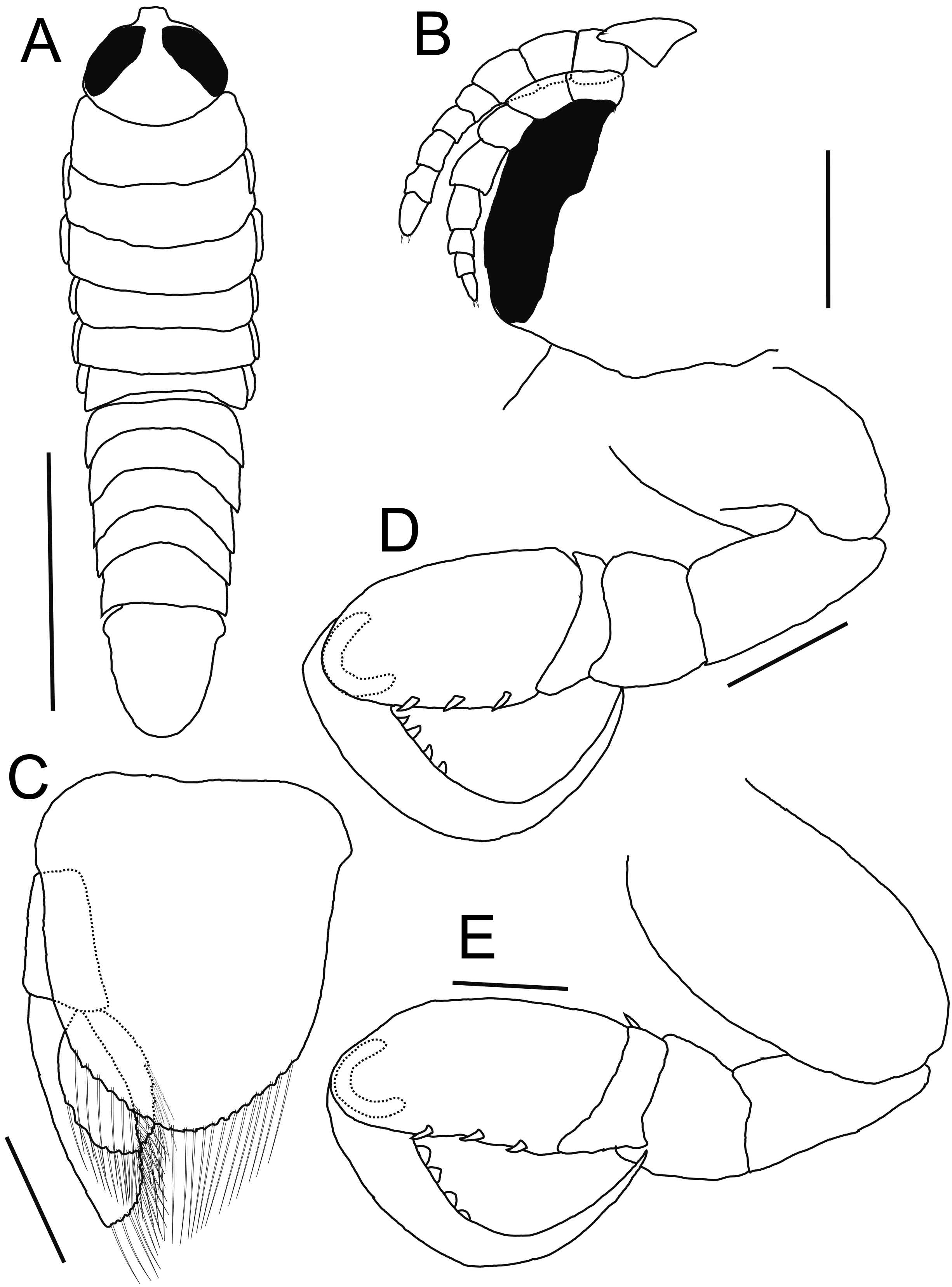


**Fig. 13.** *Mothocya parvostis* manca (3.12 mm) infesting a cobaltcap silverside *Hypoatherina tsurugae* juvenile (14.54 mm). (A) Body, dorsal view. (B) Cephalon, ventral view. (C) Pleotelson. (D, E) Pereopods 1, 2, respectively. Scale bars: A = 1 mm; B, C = 0.2 mm; D, E = 0.1 mm.

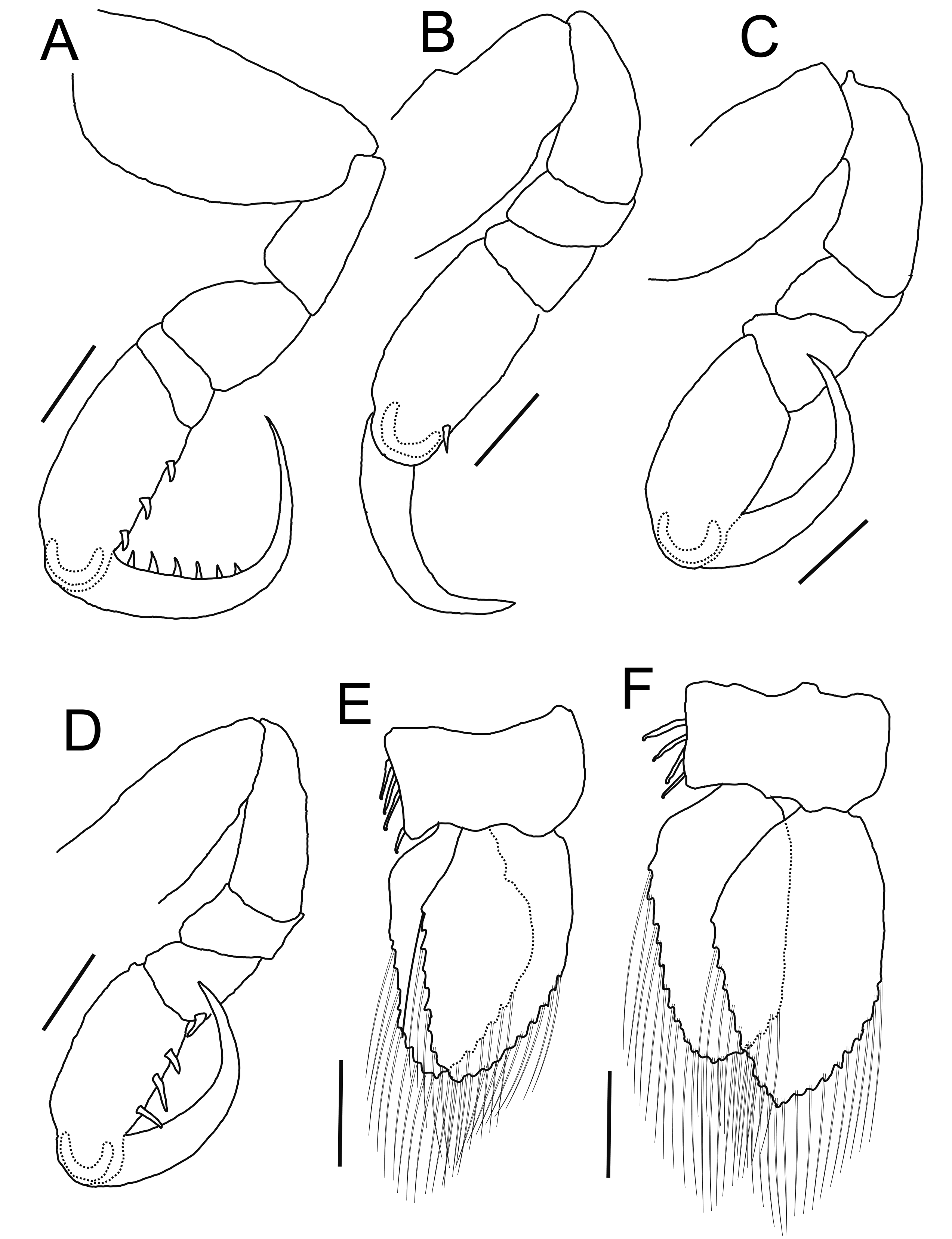


**Fig. 14.** *Mothocya parvostis* manca (3.12 mm) infesting a cobaltcap silverside *Hypoatherina tsurugae* juvenile (14.54 mm). (A–D) Pereopods 3–6, respectively. (E, F) Pleopods 1, 2, respectively. Scale bars = 0.1 mm.

Antennula with 8 articles, reaching beyond mid-point of cephalon.

Antenna with 8 articles, reaching posterior margin of cephalon.

Pereopod 1, basis 2.2 times as long as greatest width; ischium 0.5 times as long as basis; merus 0.6 times as long as ischium; carpus 0.4 times as long as merus; propodus 4.8 times as long as carpus, 3 robust setae on inferior margin; dactylus 1.2 times as long as propodus, teeth on inferior margin. Pereopod 2 similar to pereopod 1, carpus, 1 robust seta on superior distal angle. Pereopod 3 similar to pereopod 1. Pereopod 4, basis 1.8 times as long as greatest width; ischium 0.8 times as long as basis; merus 0.3 times as long as ischium; carpus 1.3 times as long as merus; propodus 2.2 times as long as carpus, 1 robust seta on inferior margin; dactylus 1.1 times as long as propodus, without teeth. Pereopod 5 similar to 4, absence of robust seta. Pereopod 6 similar to pereopod 4, carpus, 1 robust seta on inferior margin; propodus, 3 robust setae on inferior margin. No pereopod 7.

Pleopods all lamellar, surface smooth. Pleopod 1 peduncle 1.7 times as wide as length, medial margin with 4 coupling hooks; endopod trapezoidal, 1.6 times as long as width; exopod trapezoidal, lateral margin almost straight, 1.8 times as long as width, subequal length of endopod, posterior margin with long marginal setae. Pleopod 2 similar to pleopod 1; endopod without appendix masculina; exopod, 1.1 times as long as endopod.

Uropod rami beyond posterior margin of pleotelson; uropod, peduncle triangular, 0.7 times as long as exopod, 1.7 times as long as wide. Endopod oval,1.6 times as long as greatest width, 0.6 times as long as exopod, lateral and medial margins with long marginal setae. Exopod semitriangular, 3.2 times as long as greatest width, medial margin with long marginal setae.

Description of manca infesting *A. latus* (Figs. 15, 16): Similar to manca infesting *H. tsurugae*.

Pereopod 1, merus, 1 robust seta on inferior margin, 1 robust seta on superior distal angle; propodus, 2 robust setae on inferior margin; dactylus without teeth. Pereopod 2, merus, 1 robust seta on superior distal angle; carpus without robust seta; propodus, 1 robust seta on inferior margin. Pereopod 3, merus, 1 robust sera on superior distal angle; propodus, 3 robust setae on inferior margin. Pereopod 4 without robust seta and teeth. Pereopod 5, dactylus, teeth on inferior margin. Pereopod 6, carpus with 1 robust seta on inferior margin; propodus with 2 robust setae on inferior margin.

Pleopod 1 peduncle, medial margin with 3 plumose setae. Pleopod 2 peduncle, medial margin with 4 plumose setae.

Manca in blood pouch of ovigerous females infesting *H. sajori*: Similar to manca infesting *H. tsurugae* and *A. latus.*

*Remarks*: Morphological differences between mancae and juveniles of *M. parvostis* infesting *H. tsurugae* and those infesting *A. latus* were mainly found in the setations on the pereopods. The morphology of robust setae may be a key to morphological species identification for cymothoid mancae and juveniles (Saito and Fujita 2022). Morphological differences of Cymothoidae among species, growth stages, and individuals should be comprehensively examined.

Cymothoid juveniles infesting juveniles of *A. latus* and *H. tsurugae* have marginal setae on the posterior margin of the pleotelson, endopod of pleopods, and uropods, but absence of those of Juveniles infesting *H. sajori*. These marginal setae, also known as swimming setae, enhance the swimming ability of cymothoids (Tsai and Dai 1999). This indicates that juveniles infesting *A. latus* and *H. tsurugae* have better swimming ability than those infesting *H. sajori*.

## DISCUSSION

Cymothoid parasites, including *M. parvostis*, have been described on the basis of the morphological traits of adult females; thus, morphological identification is almost impossible in other life stages and in males (Fujita et al. 2021). Fujita et al. (2020) morphologically identified and described adult *M. parvostis* females infesting *H. sajori*, a major final host, and deposited their *COI* and 16S rRNA sequences into GenBank. In the present study, cymothoids were collected from *H. tsurugae* and *A. latus*, a clade that encompasses an existing sequence previously identified from *M. parvostis* (Hata et al. 2017; Fujita et al. 2020). The intraspecific genetic distances between our collections and the sequence of *M. parvostis* from GenBank were lower than the interspecific genetic distances within *Mothocya*. Thus, the cymothoid specimens collected from *H. tsurugae* and *A. latus* were identified as *M. parvostis*. *Mothocya parvostis* has been observed in the opercular cavities of *H. sajori*, *G. punctata*, and *S. quinqueradiata* as final hosts (Bruce 1986) and *A. schelgelii* as an optional intermediate host (Fujita et al. 2020). Thus, *H. tsurugae* and *A. latus* are newly identified hosts of *M. parvostis*.

In Hiroshima Bay, the spawning of *A. schelgelii*, an optional intermediate host of *M. parvostis*, peaks in early May (Kawai et al. 2017 2020 2021), and their juveniles settle in the surf zone from late June (Kawai et al. 2019). *Mothocya parvostis* mancae initially infest *A.*

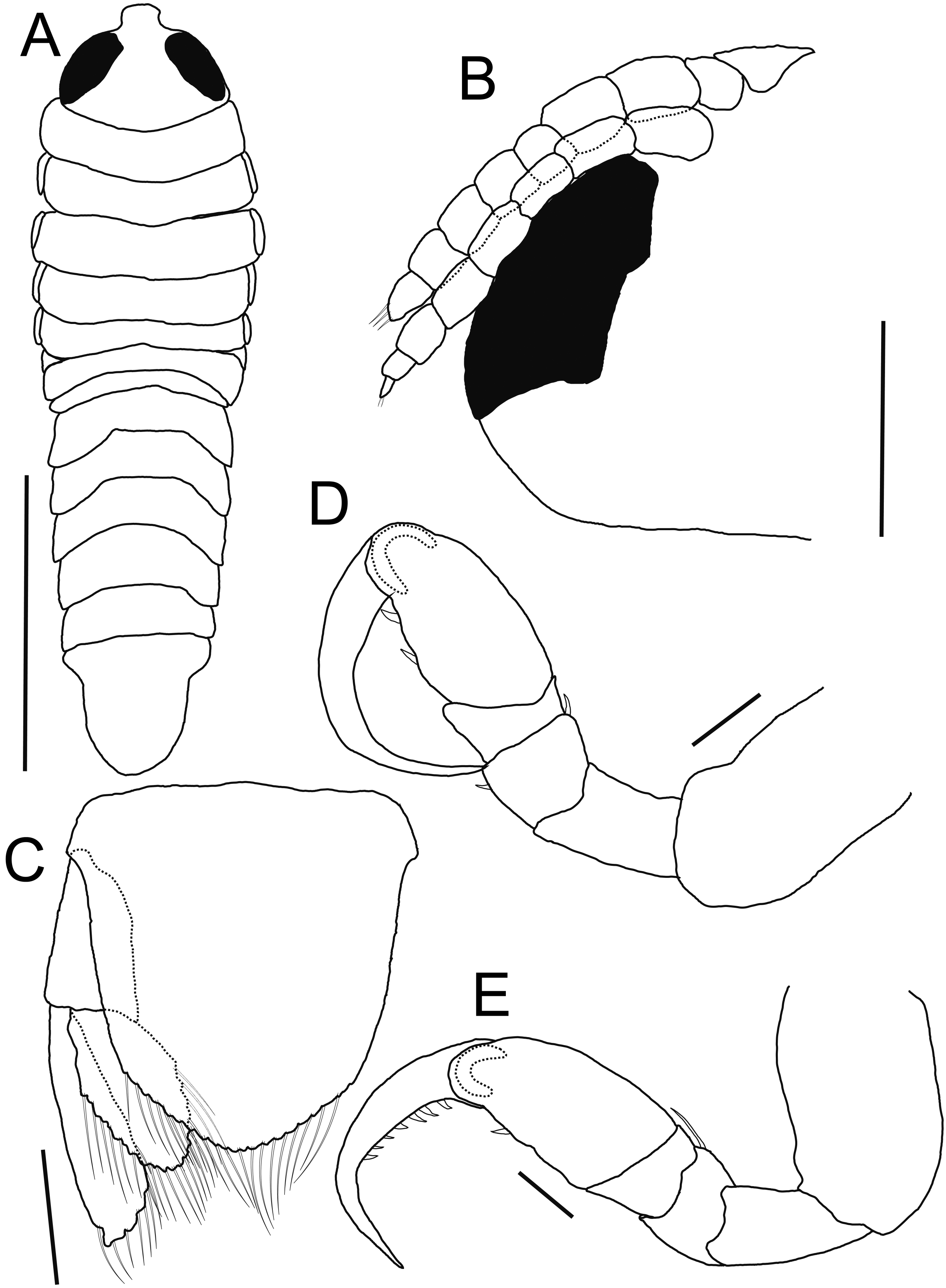


**Fig. 15.** *Mothocya parvostis* manca (2.96 mm) infesting a yellowfin seabream *Acanthopagrus latus* juvenile (12.22 mm). (A) Body, dorsal view. (B) Cephalon, ventral view. (C) Pleotelson. (D, E) Pereopods 1, 2, respectively. Scale bars: A = 1 mm; B, C = 0.2 mm; D, E = 0.1 mm.

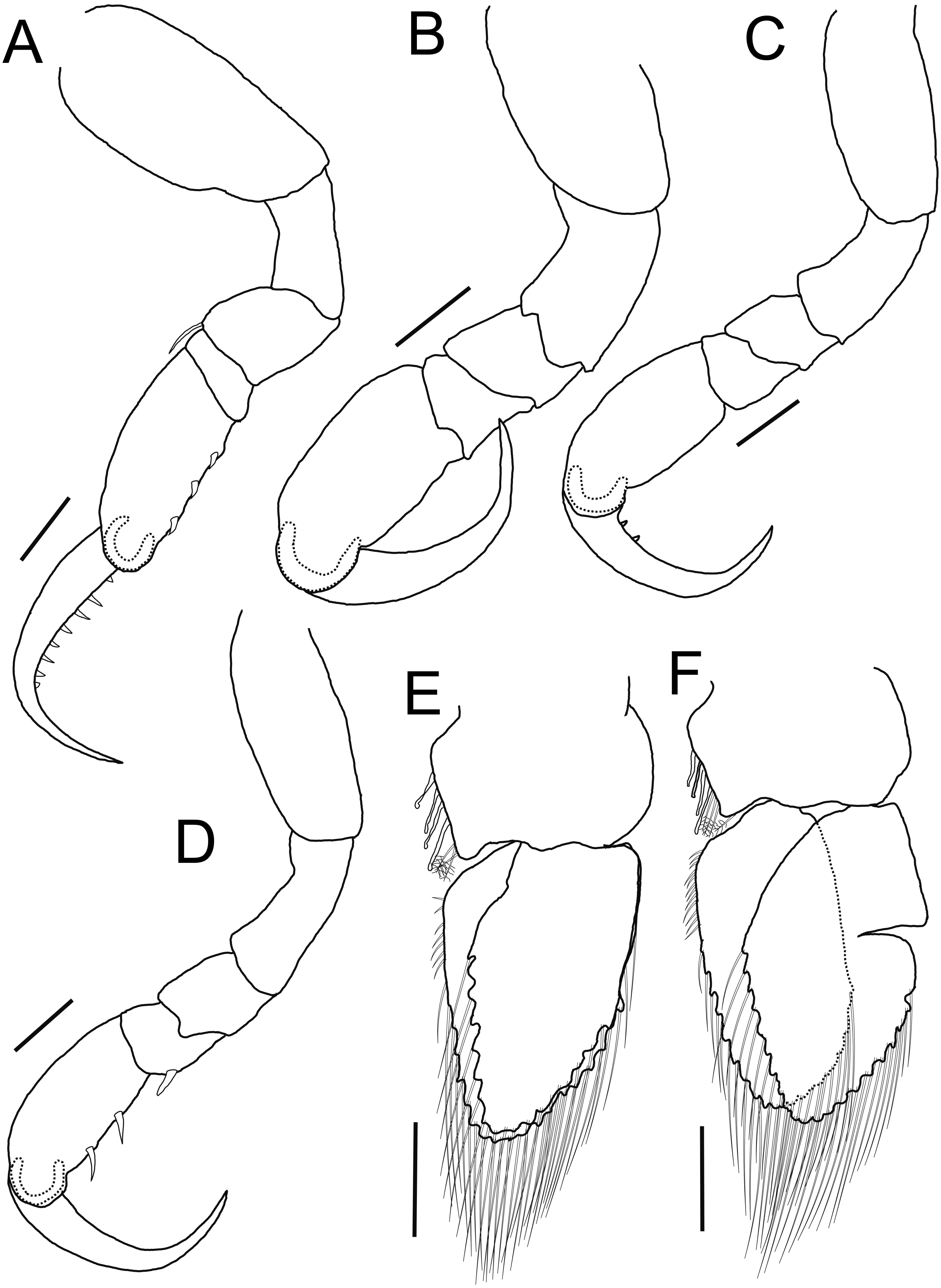


**Fig. 16.** *Mothocya parvostis* manca (2.96 mm) infesting a yellowfin seabream *Acanthopagrus latus* juvenile (12.22 mm). (A–D) Pereopods 3–6, respectively. (E, F) Pleopods 1, 2, respectively. Scale bars = 0.1 mm.

*schelgelii* juveniles after *A. schelgelii* metamorphoses and settles. Therefore, the prevalence of *M. parvostis* in *A. schelgelii* increases rapidly from late June to early August (Fujita et al. 2020). The spawning season of *H. tsurugae* in Hiroshima Bay has not been clearly determined, but it is estimated to start from May to July in other regions in Japan (Mori et al. 1988). In the present study, *H. tsurugae* juveniles were collected from July to October, a period consistent with the spawning season. The SL of *H. tsurugae* juveniles just after metamorphosis is approximately 20 mm (Tsukamoto and Kimura 1993), which is close to the minimum size of *H. tsurugae* juveniles collected in this study. In addition, their prevalence increased with each sampling day, similar to the pattern observed in *A. schelgelii*; the manca-prevalence in 10–20 mm fish was the highest. These findings suggest that *H. tsurugae* juveniles were collectively infested with *M. parvostis* mancae once metamorphosis was completed. The juvenile-prevalence was higher than the manca-prevalence in July, suggesting that *M. parvostis* mancae began infesting *H. tsurugae* juveniles before July.

The spawning season of *A. latus* in Hiroshima Bay is poorly understood, but it likely occurs in autumn (from September to November) in another region in Japan (Abol-Munafi and Umeda 1994; Nishida 2022). In the present study, *A. latus* juveniles were collected from October 2021 to January 2022, a period concordant with the spawning season. The prevalence of cymothoids during the sampling period did not significantly change, but the manca- and juvenile-prevalence changed. The manca-prevalence was higher than the juvenile-prevalence between late October and early December, but it decreased from late December and became zero in early January. The SL of *A. latus* juveniles just after they metamorphosed was approximately 10–15 mm (Tran et al. 2019), which is close to the minimum size of *A. latus* juveniles collected in this study. In addition, the manca-prevalence in fish with a size of 9–11 mm was the highest. These findings indicated that, similar to *A. schlegelii* and *H. tsurugae*, *A. latus* juveniles were collectively infested by *M. parvostis* mancae after metamorphosis.

The prevalence of *M. parvostis* in *A. schelgelii* juveniles decreases in August, and infested *A. schelgelii* juveniles are rare in September (Fujita et al. 2020). Fujita et al. (2020) stated that *M. parvostis* infestation in *A. schelgelii* juveniles is temporary and *M. parvostis* break away from *A. schelgelii* juveniles; therefore, *A. schelgelii* juveniles might be an optional intermediate host of *M. parvostis*. In *H. tsurugae* juveniles, the juvenile-prevalence increased with each sampling day, although the manca-prevalence did not significantly change. In *A. latus* juveniles, the manca-prevalence was higher than the juvenile-prevalence from October to early December, but from late December, manca-prevalence decreased and juvenile prevalence increased. By early January, all *M. parvostis* individuals infesting *A. latus* were juveniles. All parasites in small fish were mancae; in larger fish, juvenile-prevalence increased. In much larger fishes (*H. tsurugae*: ≥ 50 mm, *A. latus*: ≥ 20 mm), all *M. parvostis* individuals were juveniles. These results suggest that *M. parvostis* manca infested small *H. tsurugae* and *A. latus* juveniles. As the host fish grew, infestation was not observed. In addition, these fishes are frequently observed by humans because the two species are the subject of recreational fishing, and *A. latus* has commercial importance (Iwatsuki 2013). However, *Mothocya* infesting adult *H. tsurugae* and *A. latus* were not observed. This suggests that when infested *M. parvostis* grew with fish juveniles, the parasites left their hosts; these fish would not be suitable hosts for *M. pravostis* adults. The same pattern was observed in *A. schelgelii* (Fujita et al. 2020). Therefore, mancae and juveniles of *M. parvostis* infesting juveniles of these fishes can not mature unless they move on to infest their final hosts. Based on this finding, we conclude that *H. tsurugae* and *A. latus* are optional intermediate hosts of *M. parvostis*.

The marginal setae on the posterior margin of the pleotelson, pleopod, and uropod, also called swimming setae, enhance the swimming ability of cymothoids (Tsai and Dai 1999). Cymothoid mancae have long marginal setae for free-swimming, but generally lose them after host infestation (Smit et al. 2014). In the morphological observations in this study, *M. parvostis* juveniles infesting *H. sajori* did not have marginal setae; in contrast, *M. parvostis* juveniles infesting *H. tsurugae* and *A. latus* (optional intermediate hosts) did. Juveniles infesting *A. schlegelii* juveniles, which are optional intermediate hosts, also had marginal setae (Saito and Yoneji 2000). This indicates that *M. parvostis* juveniles lose marginal setae when infesting *H. sajori*, the final host, but may retain them when infesting the optional intermediate host. Free-swimming juveniles of *Mothocya* sp. were collected (Saito et al. 2014). This supports our hypothesis that *M. parvostis* juveniles leave optional intermediate hosts to infest *H. sajori*.

As mentioned above, the prevalence of *M. parvostis* in *A. schelgelii* juveniles rapidly increases and then decreases (Fujita et al. 2020). Similarly, the prevalence of *M. parvostis* in *H. tsurugae* juveniles increased during the sampling period. The prevalence of *M. parvostis* by SL of fish in *A. latus* was similar to that of *A. schelgelii* and *H. tsurugae*. However, the prevalence of *M. parvostis* in *A. latus* juveniles did not change significantly during the sampling period. Although the cause is unknown, this finding could be attributed to multiple factors, such as the density of mancae or the period when juveniles of fish settle. Hence, the spawning ecology of *A. latus* and the dynamics of free-swimming mancae should be determined to explain why the prevalence of *M. parvostis* in *A. latus* juveniles did not significantly change.

The reproductive cycles of cymothoid organisms vary. For example, *A. pomacentri* has no fixed reproduction season and reproduces throughout the year (Adlard and Lester 1995), but *M. epimerica* has four reproduction seasons per year (Bello et al. 1997). The reproduction cycle of *M. parvostis* is unknown, but mancae infest *A. schelgelii* juveniles from June to August (Fujita et al. 2020). *Mothocya parvostis* mancae can survive without a host for only 10–15 days (Hatai and Yasumoto 1980). Therefore, the reproductive season of *M. parvostis* must include at least June to August (Fujita et al. 2020). In this study, mancae infested *H. tsurugae* from July to October and *A. latus* from October to December. Therefore, *M. parvostis* could reproduce from June to December. Future collections of free-swimming mancae, as well as eggs and mancae from the brood pouch of ovigerous females throughout the year will help clarify the reproductive cycle of *M. parvostis*.

## CONCLUSIONS

This study and that of Fujita et al. (2020) found that *A. schelgelii*, *H. tsurugae*, and *A. latus* juveniles were infested with *M. parvostis* from June to August, July to October, and October to January the following year, respectively. In other words, optional intermediate hosts were available to *M. parvostis* for at least 8 months, and *M. parvostis* might infest different hosts depending on the time of year. Fujita et al. (2020) hypothesized that after detaching from *A. schelgelii* juveniles, *M. parvostis* juveniles can infest *H. sajori*. The results of the present study support this hypothesis, but further studies will be needed to confirm the exact life cycle. If these juveniles can infest *H. sajori* after they detach from optional intermediate hosts, using an optional intermediate host may be an excellent strategy to increase the fitness of *M. parvostis*.

**Acknowledgments:** We sincerely thank Nobuhiro Saito (Suido-sha Co. Ltd) for making helpful suggestions on drafts of this paper. We are grateful to Tatsuki Ohshita (Graduate School of Integrated Sciences for Life, Hiroshima University), Ryoya Izuta (School of Applied Biological Science, Hiroshima University), and Yuto Fujita (Faculty of Health Sciences, Hiroshima International University) for their assistance with sampling. This work was supported by JST SPRING, Grant Number JPMJSP2132. We would like to thank Editage (www.editage.com) for the English language editing. We are also grateful to two anonymous reviewers for their careful reading of our manuscript and their many insightful comments and suggestions.

**Authors' contributions:** HF designed and executed the experiments, collected samples, and wrote the manuscript. KK analyzed *A. lutas* and edited the manuscript. DD analyzed *H. tsurugae* and edited the manuscript. TU supervised and edited the manuscript. All authors have reviewed and approved the final manuscript.

**Competing interests:** HF, KK, DD, and TU declare that they have no conflict of interest.

**Availability of data and materials:** The *COI* and 16S rRNA sequences in this study were deposited into NCBI GenBank (accession numbers: LC757644–LC757691).

**Consent for publication:** Not applicable.

**Ethics approval consent to participate:** Not applicable.

## REFERENCES

Abol-Munafi AB, Ueda S. 1994. The gonadal cycle of the yellowfin porgy, *Acanthopagrus latus* (Houttuyn) reared in the net cage at Tosa Bay, Japan. Aquac Sci **42(1):**135–144. doi:10.11233/aquaculturesci1953.42.135.

Adlard RD, Lester RJG. 1995. The life-cycle and biology of *Anilocra pomacentri* (Isopoda, Cymothoidae), an ectoparasitic isopod of the coral-reef fish, *Chromis nitida* (Perciformes, Pomacentridae). Aust J Zoo **43:**271–281. doi:10.1071/ZO9950271.

Aneesh PT, Bruce NL, Kumar AB, Bincy MR, Sreenath TM. 2021. A taxonomic review of the buccal-attaching fish parasite genus *Lobothorax* Bleeker, 1857 (Crustacea: Isopoda: Cymothoidae) with description of a new species from southwestern India. Zool Stud **60:**13. doi:10.6620/ZS.2021.60-13.

Aneesh PT, Helna AK, Bijukumar A. 2019a. Redescription and neotype designation for the poorly known fish parasitic cymothoid *Joryma brachysoma* (Pillai, 1964) (Crustacea: Isopoda) from India. Folia Parasitol **66(014):**1–6. doi:10.14411/fp.2019.014.

Aneesh PT, Helna AK, Trilles JP, Chandra K. 2019b. A taxonomic review of the genus *Joryma* Bowman and Tareen, 1983 (Crustacea: Isopoda: Cymothoidae) parasitizing the marine fishes from Indian waters, with a description of a new species. Mar Biodivers **49:**1449–1478. doi:10.1007/s12526-018-0920-7.

Aneesh PT, Kappalli S. 2020. Protandrous hermaphroditic reproductive system in the adult phases of *Mothocya renardi* (Bleeker, 1857) (Cymothoidae: Isopoda: Crustacea) – light and electron microscopy study. Zool Stud **59:**61. doi:10.6620/ZS.2020.59-61.

Aneesh PT, Kappalli S, Kottarathil HA, Gopinathan A, Paul TJ. 2015. *Cymothoa frontalis*, a cymothoid isopod parasitizing the belonid fish *Strongylura strongylura* from the Malabar Coast (Kerala, India): redescription, description, prevalence and life cycle. Zool Stud **54:**1–28. doi:10.1186/s40555-015-0118-7.

Aneesh PT, Helna AK, Kumar AB, Trilles JP. 2020. A taxonomic review of the branchial fish parasitic genus *Elthusa* Schioedte & Meinert, 1884 (Crustacea: Isopoda: Cymothoidae) from Indian waters, with the description of three new species. Mar Biodivers **50:**65. doi:10.1007/s12526-020-01084-6.

Aneesh PT, Sudha K, Helna AK, Anilkumar G. 2016. *Mothocya renardi* (Bleeker, 1857) (Crustacea: Isopoda: Cymothoidae) parasitizing *Strongylura leiura* (Bleeker) (Belonidae) off the Malabar coast of India: re-description, occurrence and life cycle. Syst Parasitol **93:**583–599. doi:10.1007/s11230-016-9646-8.

Aneesh PT, Sudha K, Helna AK, Anilkumar G. 2018. *Agarna malayi* Tiwari 1952 (Crustacea: Isopoda: Cymothoidae) parasitising the marine fish, *Tenualosa toli* (Clupeidae) from India: re-description/description of parasite life cycle and patterns of occurrence. Zool Stud **57:**25. doi:10.6620/ZS.2018.57-25.

Baillie C, Welicky RL, Hadfield KA, Smit NJ, Mariani SD, Beck RM. 2019. Hooked on you: shape of attachment structures in cymothoid isopods reflects parasitic strategy. BMC Evol Biol **19(1):**207. doi:10.1186/s12862-019-1533-x.

Bello G, Vaglio A, Piscitelli G. 1997. The reproductive cycle of *Mothocya epimerica* (Isopoda: Cymothoidae) a parasite of the sand smelt, *Atherina boyeri* (Osteichthyes: Atherinidae), in the Lesina Lagoon, Italy. J Nat Hist **31(7):**1055–1066. doi:10.1080/00222939700770551.

Bleeker P. 1854. Faunae *Ichthyologicae japonicae*. Species Novae. Natuurwet Tijdschr Ned Indie **6:**395–426.

Boyko CB, Bruce NL, Hadfield KA, Merrin KL, Ota Y, Poore GCB, Taiti S, Schotte M, Wilson GDF. (eds) 2008. onwards. World Marine, Freshwater and Terrestrial Isopod Crustaceans database. Cymothoidae Leach, 1818. Accessed through: World Register of Marine Species. Available at: http://www.marinespecies.org/aphia.php?p=taxdetails&id=118274. Accessed 8 May 2022.

Bruce NL. 1986. Revision of the isopod crustacean genus *Mothocya* Costa, in Hope, 1851 (Cymothoidae: Flabellifera), parasitic on marine fishes. J Nat Hist **20:**1089–1192. doi:10.1080/00222938600770781.

Bruce NL. 1987. Australian *Pleopodias* Richardson, 1910, and *Anilocra* Leach, 1818 (Isopoda: Cymothoidae), crustacean parasites of marine fishes. Rec Aust Mus **39:**85–130. doi:10.3853/j.0067-1975.39.1987.166.

Brusca RC. 1978a. Studies on the cymothoid fish symbionts of the Eastern Pacific (Crustacea: Isopoda: Cymothoidae). I. Biology of *Nerocila californica*. Crustaceana **34:**141–154. doi:10.1163/156854078X00718.

Brusca RC. 1978b. Studies on the cymothoid fish symbionts of the Eastern Pacific (Crustacea: Isopoda: Cymothoidae). II. Systematics and biology of *Lironeca vulgaris* Stimpson 1857. Allan Hancock Occasional Papers New Series **2:**1–19.

Brusca RC. 1981. A monograph on the Isopoda Cymothoidae (Crustacea) of the eastern Pacific. Zool J Linn Soc **73:**117–199. doi:10.1111/j.1096-3642.1981.tb01592.x.

Costa A. 1851. Catalogo dei crotacei Italiani e di moltri altri del Mediterraneo per Fr. Gugl. Hope. Napoli, pp. 1–48.

Dana JD. 1852. On the classification of the Crustacea Choristopoda or Tetradecapoda. Am J Sci **2:**297–316.

Edgar RC. 2004. MUSCLE: multiple sequence alignment with high accuracy and high throughput. Nucleic Acids Res **32:**1792–1797. doi:10.1093/nar/gkh340.

Fogelman RM, Grutter AS. 2008. Mancae of the parasitic cymothoid isopod, *Anilocra apogonae*: early life history, host-specificity, and effect on growth and survival of preferred young cardinal fishes. Coral Reefs **27:**685–693. doi:10.1007/s00338-008-0379-2.

Folmer O, Black M, Hoeh W, Lutz R, Vrijenhoek R. 1994. DNA primers for amplification of mitochondrial cytochrome *c* oxidase subunit I from diverse metazoan invertebrates. Mol Mar Biol Biotech **3:**294–299.

Fujita H. 2022. Infestation of the aegathoid stage of *Anilocra clupei* (Isopoda: Cymothoidae) on a Japanese halfbeak *Hyporhamphus sajori* (Beloniformes: Hemiramphidae) collected from Japan. Cancer **31:**29–36. (in Japanese with English abstract) doi:10.18988/cancer.31.0_29.

Fujita H, Kawai K, Deville D, Umino T. 2023. Quatrefoil light traps for free-swimming stages of cymothoid parasitic isopods and seasonal variation in their species compositions in the Seto Inland Sea, Japan. Int J Parasitol Parasites Wildl **20:**12–19. doi:10.1016/j.ijppaw.2022.12.002.

Fujita H, Kawai K, Taniguchi R, Tomano S, Sanchez G, Kuramochi T, Umino T. 2020. Infestation of the parasitic isopod *Mothocya parvostis* on juveniles of the black sea bream *Acanthopagrus schlegelii* as an optional intermediate host in Hiroshima Bay. Zool Sci **37:**544–553. doi:10.2108/zs190147.

Fujita H, Umino T, Saito N. 2021. Molecular identification of the aegathoid stage of *Anilocra clupei* (Isopoda: Cymothoidae) parasitizing sweeper *Pempheris* sp. (Perciformes: Pempheridae). Crustacean Res **50:**29–31. doi:10.18353/crustacea.50.0_29.

Hata H, Sogabe A, Tada S, Nishimoto R, Nakano R, Kohya N, Takeshima H, Kawanishi R. 2017. Molecular phylogeny of obligate fish parasites of the family Cymothoidae (Isopoda, Crustacea): evolution of the attachment mode to host fish and the habitat shift from saline water to freshwater. Mar Biol **164:**1–15. doi:10.1007/s00227-017-3138-5.

Hatai K, Yasumoto S. 1980. A parasitic isopod, *Irona melanosticta* isolated from the gill chamber of fingerlings of cultured yellowtail, *Seriola quinqueradiata*. Bull Nagasaki Pref Institute Fish **6:**87–96. (in Japanese with English title)

Hesp SA, Potter IC, Hall NG. 2004. Reproductive biology and protandrous hermaphroditism in *Acanthopagrus latus*. Environ Biol Fish **70(3):**257–272. doi:10.1023/B:EBFI.0000033344.21383.00.

Houttuyn M. 1782. Beschrijving van eenige Japanse visschen en andere zee-schepzelen (Vol. 1).

Iwatsuki Y. 2013. Review of the *Acanthopagrus latus* complex (Perciformes: Sparidae) with descriptions of three new species from the Indo-West Pacific Ocean. J Fish Biol **83(1):**64–95. doi:10.1111/jfb.12151.

Jones CM, Miller TL, Grutter AS, Cribb TH. 2008. Natatory-stage cymothoid isopods: description, molecular identification and evolution of attachment. Int J Parasitol **38(3–4):**477–491. doi:10.1016/j.ijpara.2007.07.013.

Jordan DS, Starks EC. 1901. A review of the atherine fishes of Japan. Proc US Natl Mus **24:**199–206. doi:10.5479/SI.00963801.24-1250.199.

Kawai K, Fujita H, Sanchez G, Furusawa S, Umino T. 2020. Estimating the spawning season of black sea bream *Acanthopagrus schlegelii* in Hiroshima Bay, Japan, from temporal variation in egg density. Fisheries Sci **86(4):**645–653. doi:10.1007/s12562-020-01433-1.

Kawai K, Fujita H, Sanchez G, Umino T. 2021. Oyster farms are the main spawning grounds of the black sea bream *Acanthopagrus schlegelii* in Hiroshima Bay, Japan. PeerJ **9:**e11475. doi:10.7717/peerj.11475.

Kawai K, Fujtia H, Umino T. 2019. Horizontal distribution and annual fluctuations in abundance of settled juveniles of the black sea bream *Acanthopagrus schlegelii* in Hiroshima Bay, Japan. Bull Hiroshima Univ Mus **11:**1–5.

Kawai K, Okazaki R, Tomano S, Umino T. 2017. DNA identification

and seasonal changes of pelagic fish eggs in Hiroshima Bay. Nippon Suisan Gakk **83:**215–217. (in Japanese with English abstract). doi:10.2331/suisan.16-00069.
Kawanishi R, Sogabe A, Nishimoto R, Hata H. 2016. Spatial variation in the parasitic isopod load of the Japanese halfbeak in western Japan. Dis Aquat Organ **122:**13–19. doi:10.3354/dao03064.
Kimura M. 1980. A simple method for estimating evolutionary rate of base substitutions through comparative studies of nucleotide sequences. J Mol Evol **16(2):**111–120. doi:10.1007/BF01731581.
Kumar S, Stecher G, Li M, Knyaz C, Tamura K. 2018. MEGA X: molecular evolutionary genetics analysis across computing platforms. Mol Biol Evol **35(6):**1547–1549. doi:10.1093/molbev/msy096.
Latrobe BH. 1802. A drawing and description of the *Clupea tyrannus* and *Oniscus praegustator*. T Am Philos Soc **5:**77–81. doi:10.2307/1004979.
Leach WE. 1818. Cymothoadées. *In*: Cuvier, F. (Ed), Dictionnaire des Sciences Naturelles, Vol. 12. Paris, pp. 338–354.
Lindsay JA, Moran LR. 1976. Relationships of parasitic isopods *Lironeca ovalis* and *Olencira praegustator* to marine fish host in Delaware Bay. T Am Fish Soc **105:**327–332. doi:10.1577/1548-8659(1976)105%3C327:ROPILO%3E2.0.CO;2.
Martens E. 1869. Südbrasilische Süss- und Brackwasser-Crustaceen nach den Sammlungen des Dr. Reinh. Hensel. Archiv für Naturgeschichte **35:**1–37.
Mori K, Kimura S, Tsukamoto Y, Kohno Y, Yoshida M. 1988. Growth of the atherinid fish *Hypoatherina tsurugae* in Ago Bay, Central Japan. Aquac Sci **36(2):**87–90. (in Japanese). doi:10.11233/aquaculturesci1953.36.87.
Nagasawa K. 2020. *Mothocya parvostis* (Isopoda: Cymothoidae) parasitic on Japanese halfbeak, *Hyporhamphus sajori*, in the central Seto Inland Sea, Japan, with a brief summary of the hosts, geographical distribution, and pathogenic effects of the isopod. Nature of Kagoshima **47:**51–57.
Nishida Y. 2022. *Acanthopagrus latus*. *In*: Kondo Y, Ohtsuka S, Sato M. (eds) Life in the tidal flats of Hachi-no-higata: the well-preserved natural ecosystem at Takehara in the Seto Inland Sea, Japan, 1st edn. NextPublishing Authors Press, Tokyo. p. 46. (in Japanese)
Saito N, Fujita H. 2022. Morphological description and molecular barcoding of the aegathoid stage of *Nerocila japonica* Schioedte & Meinert, 1881 (Crustacea: Isopoda: Cymothoidae) infesting red seabream *Pagrus major* (Temminck & Schlegel, 1843). Crust Res **51:**47–54. doi:10.18353/crustacea.51.0_47.
Saito N, Fujita H, Aiba S. 2022. First host record of *Ceratothoa oxyrrhynchaena* (Isopoda: Cymothoidae) infesting the serranid fish, *Sacura margaritacea* (Perciformes: Serranidae). Taxa **53:**59–63. (in Japanese with English abstract). doi:10.19004/taxa.53.0_59.
Saito N, Yamauchi T, Ariyama H, Hoshino O. 2014. Descriptions and ecological notes of free-swimming forms of cymothoid isopods (Crustacea: Peracarida) collected in two waters of Japan. Crus Res **43:**1–16. doi:10.18353/crustacea.43.0_1.
Saito N, Yoneji T. 2000. The genus of *Mothocya* (Isopoda: Cymothoidae) parasitic on black sea bream juveniles *Acanthopagrus schlegelii*. Umiushi-tsushin **29:**4–6. (in Japanese).
Saitou N, Nei M. 1987. The neighbor-joining method: A new method for reconstructing phylogenetic trees. Mol Biol Evol **4:**406–425. doi:10.1093/oxfordjournals.molbev.a040454.
Schioedte JC, Meinert FW. 1881. Symbolae ad monographiam Cymothoarum Crustaceorum Isopodum Familiae 2. Anilocridae. Naturhistorisk Tidsskrift **13:**1–166.
Segal E. 1987. Behaviour of juvenile *Nerocila acuminata* (Isopoda, Cymothoidae) during attack, attachment and feeding on fish prey. Bull Mar Sci **41:**351–360.
Simon C, Frati F, Beckenbach A, Crespi B, Liu H, Floors P. 1994. Evolution, weighting, and phylogenetic utility of mitochondrial gene sequences and a compilation of conserved polymerase chain reaction primers. Ann Entomol Soc Am **87:**651–701. doi:10.1093/aesa/87.6.651.
Smit NJ, Bruce NL, Hadfield KA. 2014. Global diversity of fish parasitic isopod crustaceans of the family Cymothoidae. Int J Parasitol Parasites Wildl **3:**188–197. doi:10.1016/j.ijppaw.2014.03.004.
Taberner R, León PDR, Volonterio O. 2003. Description of the pulli stages of *Telotha henselii* (Von Martens, 1869) (Isopoda, Cymothoidae), with new hosts and locality records from Uruguay and Argentina. Crustaceana **76:**27–37. doi:10.1163/156854003321672809.
Temminck CJ, Schlegel H. 1846. Pisces. Fauna Japonica, sive descriptio animalium quae in itinere per Japoniam suscepto annis 1823-30 collegit, notis observationibus et adumbrationibus illustravit P. F. de Siebold, Parts 10–14, 173–269.
Temminck CJ, Schlegel H. 1845. *In*: Temminck and Schlegel 1843. Fauna Japonica, sive description animalium quae in itinere per Japoniam. Parts **7–9:**113–172.
Toyobo. 2012. Special feature on PCR protocols by material and application. Available at: https://lifescience.toyobo.co.jp/upload/upld99/feature/pcr99fe01.pdf. Accessed 26 May 2022. (in Japanese)
Tsai ML, Dai CF. 1999. *Ichthyoxenus Fushanensis*, New species (Isopoda: Cymothoidae), parasite of the fresh-water fish *Varicorhinus Barbatulus* from northern Taiwan. J Crust Biol **19(4):**917–923. doi:10.1163/193724099X00600.
Tran TT, Tran HD, Kinoshita I. 2019. Simultaneous and sympatric occurrence of early juveniles of *Acanthopagruslatus* and *A. schlegelii* (Sparidae) in the estuary of northern Vietnam. Limnology **20(3):**321–326. doi:10.1007/s10201-019-00581-3.
Tsukamoto Y, Kimura S. 1993. Development of laboratory-reared eggs, larvae and juveniles of the atherinid fish, *Hypoatherina tsurugae*, and comparison with related species. Jpn J Ichthyol **40(2):**261–267. doi:10.11369/jji1950.40.261.
Williams EH, Bunkley-Williams L. 1986. The 1st *Anilocra* and *Pleopodias* isopods (Crustacea: Cymothoidae) parasitic on Japanese fishes, with 3 new species. P Biol Soc Wash **99(4):**647–657.
Yamauchi T. 2016. Cymothoid isopods (Isopoda: Cymothoidae) from fishes in Japanese waters. Cancer **25:**113–119. (in Japanese with English title). doi:10.18988/cancer.25.0_113.

## Supplementary materials

**Table S1.** List of sequences from cymothoid species distributed in Japan downloaded from GenBank, with the corresponding accession numbers (Jones et al. 2008; Hata et al. 2017; Baillie et al. 2019; Fujita et al. 2020, 2021; Fujita 2022; Saito and Fujita 2022; Saito et al. 2022). (download)